

## TOPICAL REVIEW

**Collisions near threshold in atomic and molecular physics**

H R Sadeghpour<sup>†</sup>, J L Bohn<sup>‡</sup>, M J Cavagnero<sup>§</sup>, B D Esry<sup>||</sup>, I I Fabrikant<sup>¶</sup>,  
J H Macek<sup>+</sup> and A R P Rau<sup>\*</sup>

<sup>†</sup> ITAMP, Harvard–Smithsonian Center for Astrophysics, 60 Garden St, Cambridge, MA 02138, USA

<sup>‡</sup> JILA, University of Colorado, Boulder, CO 80309-0440, USA

<sup>§</sup> Department of Physics and Astronomy, University of Kentucky, Lexington, KY 40506-0055, USA

<sup>||</sup> Department of Physics, Kansas State University, Manhattan, KS 66506, USA

<sup>¶</sup> Department of Physics and Astronomy, University of Nebraska, Lincoln, NE 68588-0111, USA

<sup>+</sup> Department of Physics and Astronomy, University of Tennessee, Knoxville, TN 37996-1501 and Oak Ridge National Laboratory, PO Box 2008, Oak Ridge, TN 37831, USA

<sup>\*</sup> Department of Physics and Astronomy, Louisiana State University, Baton Rouge, LA 70803-4001, USA

E-mail: [hsadeghpour@cfa.harvard.edu](mailto:hsadeghpour@cfa.harvard.edu)

Received 4 November 1999, in final form 5 January 2000

**Abstract.** We review topics of current interest in the physics of electronic, atomic and molecular scattering in the vicinity of thresholds. Starting from phase space arguments, we discuss the modifications of the Wigner law that are required to deal with scattering by Coulomb, dipolar and dispersion potentials, as well as aspects of threshold behaviour observed in ultracold atomic collisions. We employ the tools of quantum defect and semiclassical theories to bring out the rich variety of threshold behaviours. The discussion is then turned to recent progress in understanding threshold behaviour of many-body break-ups into both charged and neutral species, including both Wannier double ionization and three-body recombination in ultracold gases. We emphasize the dominant role that hyperspherical coordinate methods have played in understanding these problems. We assess the effects of external fields on scattering, and the corresponding modification of phase space that alters the Wigner law. Threshold laws in low dimensions and examples of their applications to specific collision processes are discussed.

**1. Introduction**

When charged or neutral particles interact at low energies, at small collision velocities or in weakly bound systems, their interaction evolves over time and distance scales that are characteristically different from the usual atomic ones. The evolution from one configuration to another, i.e. clustering into atomic or molecular aggregates or fragmenting into constituents, proceeds through thresholds, e.g. excitation, ionization and dissociation limits. Particle interactions in the vicinity of a threshold thus provide the essential link between weakly bound and fragmented systems. As the de Broglie wavelength of these particles is large compared to any natural interaction length, the dynamics near threshold is amenable to analytical exploration.

Atomic physics typically focuses on sharp structures, e.g. bound states, resonances, Ramsauer minima, etc, of atoms and small molecules. Dynamics that change rather slowly with energy underly these sharp structures and can often be characterized by a few constants. The

constants are determined by atomic dynamics in a relatively small region of configuration space where all components of the atom or molecule are close together, while the sharp structures relate to large distances where the system has separated into a few fragments. For example, reflection of Schrödinger waves from a potential barrier, as occurs at negative energies, sets up standing waves at well defined energies corresponding to bound states. With a slight increase in energy, the waves can escape to infinity, but over short distances the bound and unbound waves are nearly identical, the local wavelength in this region is dominated by the strong potentials that prevail and is thereby insensitive to small changes in the energy.

Much has been learned by studying bound state energies and closely associated threshold structures in atomic and molecular physics. The study of threshold effects in atomic physics has traditionally centred on the dynamics of electron impact and electronic structure since, until very recently, only electrons and positrons had wavelengths sufficiently long for a few parameters to characterize the scattering process over an appreciable energy range. These applications are of continuing interest owing to the steady advance of techniques for controlling and detecting slow electrons and, more recently, slow positrons. The variety of atomic species available for high-resolution studies, e.g. in storage rings and traps, however, continues to increase.

Laser cooling and trapping of neutral atomic species has for the first time provided a laboratory for atomic and molecular collisions at ultracold temperatures ( $\leq 1$  mK). It is now routinely possible to probe atom–atom collisions involving only a few partial waves (often only one) of relatively long de Broglie wavelength, thus exposing the physics of threshold behaviour. It has also been established that external fields can manipulate the interaction properties of ultracold atoms and molecules. This prospect leads to fascinating modifications of threshold behaviour. The bulk of ultracold collisions involve aggregates of alkali atoms of a bosonic flavour. A recent development which truly demonstrates the dominance of threshold laws is the observation of a spin-polarized degenerate Fermi gas whose formation via *s*-wave elastic collisions is prohibited by Fermi–Dirac statistics. This allows one to peek directly into the *p*-wave threshold law in an aggregation process.

Quantum dots and surface phenomena represent other areas where threshold effects are important. Here, the threshold laws are modified by the reduced number of effective dimensions available to the Schrödinger waves. For example, the scattering length in two dimensions takes on a very different meaning than in three dimensions. Studying these differences can advance our understanding of threshold phenomena, generally.

A powerful general-purpose method which unifies the treatment of weakly bound complexes and break-up continua is the multichannel quantum defect theory (MQDT) and a variant, the multichannel effective range theory (Bethe 1949, Nath and Shaw 1965, Newton 1966). In what follows, it is observed that many of the threshold phenomena in atomic, molecular and surface physics can be analysed in the spirit of MQDT and can be parametrized in terms of a few weakly energy-dependent parameters. Despite the diversity of phenomena, threshold behaviour can always be extracted by the standard approach of Wigner's theory. This theory is most fully developed when there are only two fragments in the final state.

Threshold laws involving more than two fragments are less well understood, and, thus far, less susceptible to one unifying theoretical approach. Such laws are important for a variety of fields of physics, but particularly so in atomic physics owing to the long range of atomic forces. The celebrated Wannier threshold law for final states involving three charged particles is a notable example where standard expectations have been confounded. The rather counterintuitive results of Wannier's theory rely heavily upon classical mechanics and have not been fully brought into the general arsenal of techniques employed in quantum calculations.

The success of Wannier theory is all the more surprising since classical analysis fails to produce the Wigner law, except for the Coulomb potential.

This paper will review the standard Wigner theory for two-body final states. The diverse threshold phenomena that arise for short-range, Coulomb, dipole and polarization potentials will be discussed in section 2. Because the potentials often vary slowly with distance, the Jeffreys–Wentzel–Kramers–Brillouin (JWKB) approximation for the threshold wavefunctions will also be examined. Extension of the theory to three-body final states is the subject of section 3. Finally, threshold phenomena in lower-dimensional spaces are examined in section 4.

While there is no unifying theory for an arbitrary number of aggregates, simple phase space arguments can be used to obtain some idea of the expected behaviour. They are not rigorous and must be used with caution, but they will be mentioned here in order to set the framework for a more firmly based analysis. Consider that several particles separate to large distances. After factoring out the centre-of-mass motion, there will be several unbounded degrees of freedom,  $N = 3(N_P - 1)$ , in the case of  $N_P$  particles. We will further suppose that all coordinates have been scaled according to the corresponding particle mass so that the total energy of system  $E$  relates to the wavenumbers (we use atomic units throughout) by  $E = (k_1^2 + k_2^2 + \dots + k_N^2)/2$ . Then a cross section for any process that leads to fragmentation has the form

$$d^N \sigma = |\mathcal{M}|^2 \delta(E - (k_1^2 + k_2^2 + \dots + k_N^2)/2) dk_1 dk_2 \dots dk_N \quad (1)$$

where  $|\mathcal{M}|^2$  is the squared matrix element for the process and an energy-conserving delta function has been included. Introducing the total wavenumber  $K$  according to

$$K^2 = k_1^2 + k_2^2 + \dots + k_N^2 \quad (2)$$

and a corresponding unit vector  $\hat{\mathbf{K}}$  in  $N$  dimensions, gives

$$\begin{aligned} d^N \sigma &= |\mathcal{M}|^2 \delta(E - K^2/2) K^{N-1} dK d\hat{\mathbf{K}} \\ &= 2^{(N-2)/2} |\mathcal{M}|^2 \delta(E - K^2/2) (K^2/2)^{(N-2)/2} d(K^2/2) d\hat{\mathbf{K}}. \end{aligned} \quad (3)$$

Integrating over the wavevector  $\mathbf{K}$  gives

$$\sigma = 2^{(N-2)/2} \overline{|\mathcal{M}|^2} E^{(N-2)/2} \quad (4)$$

where the overline on  $|\mathcal{M}|^2$  denotes an angle average.

The key ingredient of simple phase space arguments is the assumption that, in the absence of any evidence to the contrary, the average matrix element is essentially constant over small ranges of  $E$  near  $E = 0$ . Equation (4) then gives the standard threshold law that cross sections are proportional to  $E^{(N-2)/2}$ . For example, if  $N = 3$ , we recover the usual  $E^{1/2}$  threshold law for two bodies, while for  $N = 6$ , one obtains the expected  $E^2$  behaviour for three-particle fragmentation.

Long-range potentials, most notably Coulomb or dipole interactions, induce characteristic energy dependences in the matrix element, thereby altering the phase space threshold laws. Polarization and other interactions with potentials that drop off faster than  $r^{-2}$  do not usually change inelastic threshold laws, but they often imply that the phase space law has only a very short range of validity. The asymptotic waves for all such potentials are known analytically, and an approximate description through the JWKB approximation often suffices. Such ‘Wigner threshold laws’ are well established for two-body final states and can be employed with considerable confidence in new physical situations. Section 2 reviews this subject in the context of atomic physics.

Theories for multi-particle fragmentation are much less well developed, with no rigorous method that can be applied in all cases. Even the  $E^2$  law for short-range potentials must be

qualified for the exceptional case where the two-body s-wave scattering length  $a_s$  is infinite. When  $a_s \rightarrow \infty$ , the three-body break-up threshold cross section becomes singular owing to an effect discussed by Thomas (1935) and later by Efimov (1970). When the fragments are charged, the threshold law was obtained by Wannier using semiclassical analysis, but the law has never been proven in the sense that Wigner's threshold laws have been. Section 3.1 outlines a derivation of Wannier's threshold law and discusses some of its limitations.

For three or more particles, there is no widely accessible JWKB approximation. While Feynman's semiclassical propagator forms the basis for such approximations in principle, it is too difficult to employ generally for many particles, owing to the possibility of chaotic motion. Even so, valuable insights have emerged from the classical theory, in particular concerning the range of validity of threshold laws. Alternatives that do not employ classical orbits directly include a multi-crossing model discussed in section 3.1.2, and also a hidden-crossing theory, familiar from ion–atom collisions. Three neutral particles interacting via short-range forces can be described in hyperspherical coordinates whose asymptotic properties are readily exploited using Wigner's analysis for short-range interactions. The proviso here is that the ordinary radial coordinate is replaced with the hyper-radius, as in section 3.2.

External fields often freeze out some electronic degrees of freedom in atoms and molecules, which would otherwise be available to the electrons, as with the transverse motion of electrons in atoms in strong magnetic fields, and with trapped electrons in mesoscopic devices, such as quantum dots. Phase space arguments must be modified. Derivation of the threshold phenomena in one and two dimensions is included in section 4.

## 2. Two-body threshold laws

A complete development of two-body threshold behaviour was given by Wigner (1948) over 50 years ago, emphasizing that the longest-range forces govern the energy dependences of observables near threshold. As in other developments Wigner made, such as the  $R$ -matrix theory, the interaction between the two bodies is usefully separated into small and large  $r$ , where  $r$  is the separation distance. The key point is that the energy  $E$  in the relevant channel, when it lies just above threshold ( $E = 0$ ), is a significant parameter only at asymptotically large  $r$ . At small  $r$ , in contrast, when the bodies are close together and interacting strongly, the potentials that prevail completely dwarf  $E$ . Thereby, the local wavenumber in that region is insensitive to small changes in  $E$ , depending instead on those strong potentials. It is only when the bodies separate to large  $r$  and these potentials drop off, particularly as  $r \rightarrow \infty$ , that  $E$  and its associated asymptotic wavenumber  $k$  in the channel ( $E = k^2/2$  in atomic units) become significant. Therefore, sensitive dependences of the cross section  $\sigma$  on  $k$  near threshold can only arise at large  $r$ . Indeed, by the same token, it is the longest-range potential in that channel that will dominate the behaviour of  $\sigma$  closest to threshold.

This makes the study of threshold behaviour easier than seeking a full solution of the problem, skirting the complexities of the small- $r$  region. At the same time, threshold behaviour is a useful diagnostic of the long-range potentials in the problem.

### 2.1. Short-range potentials

Once the particles have traversed Wigner's threshold zone, a small- $r$  region where the two-body potential is dominant, the probability of escape of fragments is determined by the phase space available at the energy  $E$  for the particles to escape to infinity (see section 1). As discussed earlier, with  $N_p = 2$  and  $N = 3$ , the threshold behaviour for an inelastic differential cross section is  $\sigma(k) \equiv (d\sigma/dE) \propto k^2(dk/dE) = k$ , a linear  $k$  dependence. For elastic scattering, it

is the phase shift that has this  $k$  dependence. Corresponding phase space dependences govern threshold behaviour in other dimensions (see section 4).

For channels with non-zero orbital angular momentum  $\ell$ , as is often the case in atomic and molecular systems, the ‘angular momentum potential’ (or ‘centrifugal barrier’)  $\ell(\ell + 1)/2r^2$  forms an effective long-range potential. Indeed, its  $1/r^2$  dependence is what marks the separation between short- and long-range regions for external potentials, any that fall off faster (slower) than  $1/r^2$  belonging to the former (latter) category. In the case of short-range potentials, this angular momentum term provides the longest-range potential and governs the threshold behaviour (section 2.5). Two equivalent views of the  $1/r^2$  behaviour lead to an additional  $k^\ell$  dependence in the matrix element contributing to the phase shift or cross section. One view of tunnelling through the angular barrier in going from the reaction zone to infinity will be considered in section 2.6, but here we turn to a more direct picture. The relevant dimensionless combination being  $kr$ , the ‘suppression’ in the amplitude at small  $r$  of a wavefunction with non-zero  $\ell$ , namely  $r^\ell$ , translates into a  $k^\ell$  in any matrix element involving such a wavefunction. Thereby, the threshold behaviour, consistent with equation (3), becomes

$$\begin{aligned} d\sigma_{\text{inel}}/dE &\propto k^{2\ell+1} \\ \tan \delta_{\text{el}} &\propto k^{2\ell+1} \end{aligned} \quad (5)$$

considered as the standard Wigner threshold laws for short-range potentials (Wigner 1948). Together with a kinematic  $1/k^2$  factor, an elastic cross section has the dependence  $\sigma_{\text{el}} \propto k^{4\ell}$ .

Stripped down to its barest essentials, the Wigner argument leading to the results in equation (5) is as follows (section 132 of Landau and Lifshitz 1977, Rau 1984a). Outside the radius  $r_0$  of the short-range potential, the radial Schrödinger equation exactly at  $E = 0$  has only the kinetic energy terms, the radial kinetic energy and angular momentum potential. Therefore, the general solution is

$$R_\ell(E = 0) = A_1 r^\ell + A_2 r^{-(\ell+1)} \quad (6)$$

with  $A_1$  and  $A_2$ , particularly the ratio  $A_1/A_2$ , having no dependence on  $E$ . At these same distances  $r > r_0$ , at  $E > 0$ , the Schrödinger equation being homogeneous in the combination  $kr$ , the solution

$$R_\ell(E) = (\text{regular}) - \tan \delta_\ell (\text{irregular}) \quad (7)$$

must, for smooth and continuous matching to equation (6), be of the form

$$R_\ell(E) = (kr)^\ell + \tan \delta_\ell (kr)^{-(\ell+1)} \quad (8)$$

with

$$\tan \delta_\ell = (A_2/A_1)k^{2\ell+1} \quad R_\ell(E) = k^\ell R_\ell(E = 0) \quad (9)$$

giving the results in equation (5). This argument does not require any detailed knowledge of the regular and irregular solutions involved and will be adapted in sections 2.5 and 3 for more complicated potentials.

## 2.2. Coulomb potential

The  $Z/r$  Coulomb interaction between two charged bodies is long range relative to angular momentum and, indeed, the longest-range potential encountered in atomic and molecular physics. The dependences in equation (5) are completely modified as is obvious because  $\ell$  ceases to be a significant parameter, the  $1/r$  potential and not  $\ell(\ell + 1)/2r^2$  being dominant

at infinity. Wigner had already in his classic paper (Wigner 1948) worked out these Coulomb threshold laws. In addition to the phase space factor,  $k$ , the suppression (enhancement) of the squared wavefunction at small  $r$  in the case of repulsive (attractive) Coulomb interaction is  $(1/k) \exp(-\pi Z/k)$  and  $1/k$ , respectively, and independent of  $\ell$  (p 566 of Landau and Lifshitz 1977). Therefore, for the attractive Coulomb potentials, the inelastic cross sections and elastic phase shifts become constant, independent of energy and angular momentum near threshold. Inelastic thresholds open with a finite, non-zero jump in the cross section at threshold. A useful insight into the occurrence for all  $\ell$  is provided by considering the region just below threshold which, in such a Coulomb system, has an infinite pile-up of Rydberg states with arbitrarily high  $\ell$ . An energy average over the resonant excitation of these states gives the non-zero value that extrapolates above threshold as a similar constant cross section (Gailitis 1963, Seaton 1983, figure 2.1 of Fano and Rau 1986).

The energy independence of the cross section at threshold for attractive Coulomb potentials is connected to the existence of a so-called ‘Coulomb zone’, a region stretching over a large range of  $r$  in which the Coulomb potential dominates over the kinetic energy. Over this entire region, the local wavelength of the wavefunction’s oscillations is independent of  $E$ , being determined by  $Z$  alone (section 36 of Landau and Lifshitz 1977). Only past  $r > Z/E$  lies the ‘far zone’ with oscillations governed by the wavelength  $1/k$ . As  $E \rightarrow 0$ , the Coulomb zone covers the entire asymptotic range and the energy dependence drops out of the wavefunction and the threshold law. At the same time, the JWKB approximation applies in the Coulomb zone and describes in common the continuum and bound states for  $E \approx 0$ .

### 2.3. Effective range expansions

To go further than the leading energy dependence of the Wigner threshold laws as in equation (5), the same division between small and large  $r$  proves crucial. Thus, the first relation in equation (9) may be viewed as expressing an expansion of  $k^{2\ell+1} \cot \delta_\ell$  near threshold, the leading term being constant in energy,  $(A_1/A_2)$ , with further terms involving higher powers of  $E$ . For  $\ell = 0$ , this gives Wigner’s effective range expansion introduced in the early days of nuclear physics,  $k \cot \delta_0 = -(1/a) + r_{\text{eff}} E + \dots$ , where  $a = -(A_2/A_1)$  is the scattering length and  $r_{\text{eff}}$  the ‘effective range’ (Bethe 1949, Newton 1966).

Subsequently, multichannel quantum defect theory in atomic and molecular physics has interpreted these results as follows (Seaton 1983, Fano and Rau 1986). At small  $r$  ( $> r_0$ ), the radial wavefunction and the parameters therein can be defined with no reference to the asymptotic energy  $E$ . Thus from equation (6),  $R_0(E = 0) = A_1(1 - a/r)$  with  $a$  independent of  $E$ , and even the normalization  $A_1$  can be similarly chosen. The scattering length  $a$  is determined by matching logarithmic derivatives of this solution, valid just outside  $r_0$ , to that of the interior solution within the reaction zone which starts at the origin as  $r^\ell$ .

The scattering length can be regarded, therefore, as a ‘smooth, short-range phase shift’,  $\tan \delta_0^0 = -a/r_0$ , the superscript zero on quantities indicating insensitivity to  $E$ . The physical phase shift  $\delta_\ell$  in equation (7), on the other hand, is defined at asymptotic  $r$  with reference to regular and irregular functions defined at large  $r$  including their normalization, typically chosen as normalization per unit energy. All sensitive energy dependences are contained therein so that the factor  $k$  (or, more generally,  $k^{2\ell+1}$ ) in equation (5),  $\tan \delta_0 = (kr_0)(-a/r_0) = (kr_0) \tan \delta_0^0$ , translates the smooth phase shift defined at small  $r$  to the energy-dependent physical phase shift at infinity.

Such translations through the parameter called  $\mathcal{B}$  in MQDT, which is essentially  $(kr_0)^{2\ell+1}$ , are codified not just for the phase shift but for the regular and irregular functions themselves and all the other scattering quantities which depend on them. A base pair of regular and irregular

solutions  $(f^0, g^0)$  for any long-range field, defined at small  $r$  and insensitive to energy, are related to a corresponding pair  $(f, g)$ , appropriate to asymptotic distances and normalized per unit energy, through

$$\begin{pmatrix} f \\ g \end{pmatrix} = \begin{pmatrix} \mathcal{B}^{1/2} & 0 \\ \mathcal{B}^{1/2}\mathcal{G} & \mathcal{B}^{-1/2} \end{pmatrix} \begin{pmatrix} f^0 \\ g^0 \end{pmatrix} \quad (10)$$

where  $\mathcal{G}$  is another MQDT parameter, not essential for our purposes here. Note that  $\mathcal{B}^{1/2}$ , which reduces to the  $k^{\ell+1/2}$  in equation (5), links the normalizations appropriate to small and large  $r$ . Counterpart relations below threshold, involving a parameter  $\mathcal{A}$  in place of  $\mathcal{B}$ , occur in MQDT but are ignored here, although they are useful for extrapolating to negative energies (see chapters 4 and 5 of Fano and Rau 1986).

The connection between the asymptotic phase shifts and the smooth, short-range ones is provided by the relations obtained from equation (10),

$$\begin{aligned} \tan \delta_\ell^0 &= \mathcal{B}^{-1/2} \tan \delta_\ell [\mathcal{B}^{1/2} - \mathcal{B}^{-1/2}\mathcal{G} \tan \delta_\ell]^{-1} \\ \tan \delta_\ell &= \mathcal{B} \tan \delta_\ell^0 [1 + \mathcal{G} \tan \delta_\ell^0]^{-1}. \end{aligned} \quad (11)$$

Thus, once the parameters  $\mathcal{B}$  and  $\mathcal{G}$  are catalogued for any long-range potential, as they have been (table 5.1 of Fano and Rau 1986), one can pass back and forth between the two phase shifts. In particular,  $\tan \delta_\ell^0$  obtained from matching to solutions in the reaction zone (or from Wigner's  $R$ -matrix) can be expanded as a slowly varying function in powers of  $E$ , and the second equation in equation (11) then gives the full effective range expansion for  $\tan \delta_\ell$  with all its possibly complicated energy dependences arising from the parameter  $\mathcal{B}$  (and, to a lesser extent,  $\mathcal{G}$ ).

The above single-channel treatment extends to many channels. Consider an  $N$ -channel system and introduce the multichannel wavefunction in the form of an  $N \times N$ -matrix  $\psi$  which has the following form outside the reaction sphere,  $r > r_0$ ,

$$\psi = h^{(-)} - h^{(+)} S \quad (12)$$

where  $S$  is the scattering matrix and  $h^{(\pm)}$  are channel wavefunctions with travelling-wave behaviour. They are linear combinations of the standing waves  $(f, g)$  and have the following asymptotic behaviour:

$$h_{ij}^{(\pm)} \sim \delta_{ij} k_i^{-1/2} \exp[\pm i(k_i r - l_i \pi/2)] \quad (13)$$

where  $k_i$  and  $l_i$  are linear and angular momenta in channel  $i$ . The asymptotic form in equation (13) assumes that all  $N$  channels are open. However, the whole treatment can be easily generalized if there are  $N_c$  additional closed channels. The corresponding diagonal matrix elements of  $h^{(+)}$  behave like  $e^{-|k_i|r}$ , and the matrices  $h^{(-)}$  and  $S$  become rectangular with  $N + N_c$  rows and  $N$  columns. For the sake of simplicity, we will not dwell further on details related to closed channels (see chapters 7 and 8 of Fano and Rau 1986).

The partial (for a given set of angular momenta) cross section for transition from initial state  $i$  to a final state  $f$  is proportional to  $|T_{fi}|^2$ , where  $T$  is the transition matrix related to the scattering matrix  $S = I - T$ , with  $I$  the identity matrix. The function  $\psi$  is matched with the internal wavefunction in the form

$$\psi = R \frac{d\psi}{dr} \quad (14)$$

where  $R$  is the Wigner  $R$ -matrix, a meromorphic function of energy with poles only on the real axis. In deriving the threshold laws, we assume that  $R$  depends weakly on energy. A special treatment is necessary if there is a bound, a virtual or a resonance state near the threshold.

Solving equation (14) for  $S$ , we obtain finally the equation of Ross and Shaw (1961),

$$T = -2ik^{l+1/2}(M - ik^{2l+1})^{-1}k^{l+1/2} \quad (15)$$

where  $M$  depends on  $R$  and is also a meromorphic function of energy. This equation allows us to obtain threshold laws for elastic and inelastic processes. In particular, the Wigner threshold law for an inelastic process is

$$T_{fi} \sim k_f^{l_f+1/2}. \quad (16)$$

Furthermore, assuming that all poles of the  $M$ -matrix are far from the threshold, we can expand  $M$  in powers of  $k_f^2$  and obtain the effective range expansion for all transition matrix elements near threshold. If  $\det M$  has a zero near threshold, we have the case of near-threshold resonance scattering.

The case of the Coulomb interaction in the final state can be treated similarly by substituting the Coulomb functions for  $h^{(\pm)}$ . As a result, the cross section for inelastic processes becomes finite at threshold in the case of attraction and exponentially small in the case of repulsion.

#### 2.4. Dipole potential

The dipole potential is of the form  $-D/r^2$ , where  $D$  can be either positive (attractive dipole) or negative (repulsive dipole). A polar molecule presents an instance, as also does any excited atom with a degenerate  $\ell$  manifold, for an incoming charge. When the dipole is combined with the centrifugal potential, the resulting effective potential,  $\lambda(\lambda+1)/r^2$ , will have complex angular momenta  $\lambda = -\frac{1}{2} + i\alpha$ , when  $D > D_{\text{cr}}$ . Here,  $\alpha = \sqrt{2D - (\ell + \frac{1}{2})^2}$  and  $D_{\text{cr}} = \frac{1}{2}(\ell + \frac{1}{2})^2$ . The MQDT parameters are available (see chapter 5 of Fano and Rau 1986, Greene *et al* 1979) and, as in the case of the Coulomb field, inelastic cross sections start with a finite step at threshold (with an additional slow oscillation in  $k$ ). Again in this situation, there is correspondingly an infinity of dipole-bound states below the threshold (see section 35 of Landau and Lifshitz 1977, Greene and Rau 1985, Hino and Macek 1996).

**2.4.1. Degenerate channels.** Due to conservation of parity, the dipolar interaction is non-diagonal in angular momentum, so that the problem is always a multichannel one even outside the reaction sphere. Fortunately, the dipolar interaction exhibits the same long-range behaviour as the centrifugal potential. If the dipolar interaction couples channels with the same energy, the problem is reduced to the diagonalization of the matrix

$$A = \ell(\ell + 1) - 2D \quad (17)$$

where  $D$  is the dipole moment matrix obtained by calculating the matrix element of dipolar interaction between angular momentum eigenstates. Two cases of practical importance are electron-impact excitation of the hydrogen atom and scattering by non-rotating polar molecules. In the first case, the matrix  $D$  has a finite size due to conservation of the total angular momentum of the system. Methods for the diagonalization and classification of eigenvalues are discussed in Herrick (1975), Nikitin and Ostrovsky (1978) and Gailitis (1982). In the second case, the size of the matrix  $A$  is infinite but its eigenvalues rapidly converge in all cases of practical importance. In both cases, the assumption of degenerate channels, which is necessary to have an induced dipole moment, involves an approximation: we assume that the Lamb shift (for collisions with hydrogen atoms) or rotational spacing (for collisions with polar molecules) is small compared to the electron energy. Necessary modifications for lower

energies for electron–molecule scattering will be discussed in the next section. Other cases involving collisions with muonium and other heavy particles were discussed by Gailitis (1982).

Diagonalization of the matrix  $A$  allows us to express the solution of the Schrödinger equation outside the reaction sphere as a linear combination of Bessel functions with indices  $\lambda_i + \frac{1}{2}$ , where  $\lambda_i$  are related to the eigenvalues  $\Lambda_i$  of  $A$  through  $\Lambda = \lambda(\lambda + 1)$ . Then the  $R$ -matrix matching condition can be applied in the same way as in the case of short-range interactions. The final result is conveniently expressed in terms of a matrix  $S'$  which is connected to  $S$  by a non-unitary transformation (Gailitis and Damburg 1963),

$$S = \exp(i\pi l/2)U \exp(-i\pi\lambda/2)S' \exp(-i\pi\lambda/2)U^{-1} \exp(i\pi l/2) \quad (18)$$

where  $U$  is the orthogonal matrix which diagonalizes  $A$ . Then for  $S'$  we obtain (Gailitis and Damburg 1963, Fabrikant 1977)

$$S' = 1 + 2ik^{\lambda+1/2}\{M - (\tan \pi\lambda + i)k^{2\lambda+1}\}^{-1}k^{\lambda+1/2}. \quad (19)$$

The form of the threshold law depends critically on the lowest eigenvalue  $\Lambda_0$ . If  $\Lambda_0 > -\frac{1}{4}$ , all  $\lambda_i$  are real, the  $T$ -matrix element for the inelastic process is proportional to  $k^{\lambda_0+1/2}$  and the cross section becomes proportional to  $k^{2\lambda_0+1}$ . If  $\Lambda_0 < -\frac{1}{4}$ ,  $\lambda_0 + \frac{1}{2}$  is pure imaginary, and the cross section is finite at the threshold. This occurs at all excitation thresholds in the case of the hydrogen atom. In the case of scattering by polar molecules, this happens if the dipole moment exceeds the critical value  $D_{\text{cr}} = 0.6395$  atomic units (au). In this case, the major energy dependence of the cross section is given by the denominator of equation (19). In particular, the cross section for inelastic processes with the dipolar interaction in the final state can be written as (Fabrikant 1977, 1978) ( $k \equiv k_f$ )

$$\sigma_{fi} = \frac{\text{constant}}{|e^{-i\beta} + e^{\pi\alpha}k^{2i\alpha}|^2} \quad (20)$$

where  $\alpha = \text{Im } \lambda$  and the parameter  $\beta$  depends on elements of the  $M$ -matrix as well as on the dipole moment.

Although  $\beta$  is generally complex, its imaginary part is small if interactions with other channels (other than dipole-coupled near-threshold channels) is weak. In particular,  $\beta$  is real for pure elastic scattering. In this case, analytic continuation of the  $T$ -matrix below the threshold into the region of negative  $k_f^2$  allows us to find the poles whose positions are given by the equation

$$k^2 = -\exp\{-[\pi(2n + 1) + \beta]/\alpha\} \quad n = 0, 1, \dots \quad (21)$$

These are, of course, the well known dipole-supported states discussed originally by Fermi and Teller (1947). Note that these states converge rapidly (exponentially) to the threshold. The rotational splitting reduces the number of these states from infinity to a finite number, sometimes even to zero. For example, the HF and H<sub>2</sub>O molecules have supercritical dipole moments; however, they do not have stable anion states. Crawford and Garrett (1977) concluded that a dipole-supported state remains bound after inclusion of rotation if its fixed-nuclei binding energy exceeds a tenth of the rotational constant.

If there are open channels below threshold, the bound states become dipole-supported Feshbach resonances. They have been observed in photodetachment experiments (Jackson *et al* 1979, Lykke *et al* 1984). If the vibrational motion of the molecule is included, each dipole-supported state can generate a series of vibrational Feshbach resonances, originally called ‘nuclear-excited’ Feshbach resonances (Bardsley and Mandl 1968). A pronounced vibrational Feshbach resonance below the first vibrational excitation threshold was recently observed (Hotop *et al* 1995, Schramm *et al* 1999) in the process of dissociative electron attachment

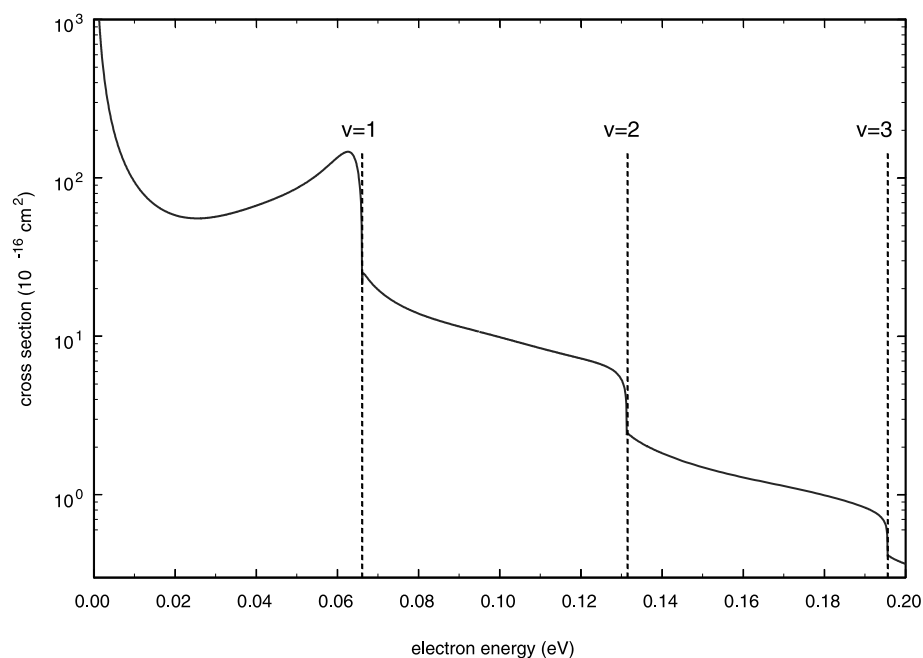


**Figure 1.** Calculated cross section for dissociative attachment in collisions of low-energy electrons with  $\text{CH}_3\text{I}$  molecules in the ground vibrational state. The thresholds for vibrational excitation of the symmetric C–I stretch mode are shown by broken vertical lines.

to the methyl iodide molecule. The dipole moment of methyl iodide,  $D = 0.638$  au, is not strong enough to support a bound state. It was shown (Schramm *et al* 1999) that this resonance is mediated by the combined effect of the dipolar and polarization interactions. In figure 1 we present the theoretical dissociative attachment cross section. In addition to the vibrational Feshbach resonance, a very pronounced cusp structure (a discontinuity of the derivative of the cross section in energy) is seen at the first and second thresholds. The theory of the threshold cusps based on analyticity and unitarity of the  $S$ -matrix was developed by Baz' (1957). They result directly from equation (15) which is due to Ross and Shaw (1961). We should note, however, that the original theory of the cusp structure should be modified (Fabrikant 1977) to include the effects of the dipolar interaction. In  $\text{H}^-$  (Bryant *et al* 1977, Harris *et al* 1990), the Feshbach resonances are associated with simultaneous excitation of two electrons below each manifold of degenerate detachment threshold. The binding of these resonances occurs due to the attractive induced dipole potentials which form because of the accidental degeneracy of hydrogen angular momentum states.

Above threshold, the analytical structure of equation (20) leads to oscillations of the cross section as a function of energy. However, these oscillations cannot be observed in practice (Fabrikant 1977); see also Greene and Rau (1985) for a similar discussion involving three bodies in section 3. If the dipole moment is just larger than the critical value, the period of oscillations exceeds the rotational spacing, whereas for higher dipole moments the amplitude of oscillations becomes exponentially small.

Turning to the more complicated example of a rotating dipole, we must distinguish between two cases. In the first case, rotation removes all degeneracies of the dipole-coupled channels.

In the second case, degenerate channels coupled by the dipolar interaction still remain. The second case is typical of symmetric-top molecules.

*2.4.2. Diatomic and non-symmetric polyatomic molecules.* If the electron energy in the final state is small compared to the rotational spacing, the dipole coupling becomes equivalent to the action of a diagonal potential which, in the case of electron–atom collisions, behaves at large distances as a polarization potential  $-\beta/2r^4$  (note that  $\beta$  can be both positive and negative). In the case of scattering by polar molecules the long-range behaviour of the effective diagonal potential depends on the total angular momentum  $J$ . If  $J = 0$ , the effective polarizability is given by (Clark 1979, Fabrikant 1983)  $\beta = D^2/3B$  where  $B$  is the rotational constant. For  $J > 0$  and s-wave electrons, the effective static polarizability vanishes, and the long-range behaviour is determined by the dynamical polarization decaying as  $r^{-6}$ . In all cases, the Wigner threshold law is restored. It is also possible to find an analytical correction to the Wigner law of the order of  $\beta k_f^2 \ln k_f$  (Damburg 1968, Gailitis 1970).

The region of transition between the Wigner law and the dipole threshold law is much more complicated. Even in the simplest two-channel case, the solution has a very complicated analytical structure (Gailitis 1970). Therefore, most of the studies in this region were performed by numerical integration of the coupled equations (Fabrikant 1978, 1983).

An interesting situation occurs when the dipole moment of the molecule is supercritical, that is, the fixed-nuclei approximation leads to the appearance of dipole-supported states. When the rotational splitting is included, all or most of them disappear because of the effective cut-off of the dipole potential. As just discussed, at large distances the effective electron–dipole interaction decays as  $r^{-4}$  or even faster. At shorter distances, where the rotational spacing is smaller than the electron–dipole interaction, the adiabatic body-frame representation (Clark 1979, Fabrikant 1983) is more appropriate. In this region, the dipole potential leads to binding and anisotropy of the electron wavefunction. The size of the inner (adiabatic) region may be as large as a few hundred au. It means that the dipolar interaction may be strong enough to create a diffuse bound or a virtual state (Frey *et al* 1994). In particular, very diffuse virtual states were found in electron scattering by HF (Hill *et al* 1996) and CH<sub>3</sub>Cl (Frey *et al* 1995, Fabrikant and Wilde 1999).

In the presence of a nearby bound or virtual state, the  $S$ -matrix element for transition  $i \rightarrow f$  behaves as ( $k \equiv k_f$ )

$$S_{fi} \sim \frac{k^{l_f+1/2}}{k - i\kappa}. \quad (22)$$

The position of the  $S$ -matrix pole is given by  $k = i\kappa$ , where  $\kappa$  is positive in the case of a bound state and negative in the case of a virtual state. In collisions when  $l_f = 0$  dominates, we obtain for the excitation cross section (see section 143 of Landau and Lifshitz 1977)

$$\sigma_{fi} = \frac{ak}{k^2 + \kappa^2} \quad (23)$$

where  $a$  is a constant. Equation (23) actually assumes that the interchannel coupling is weak. However, the dipolar coupling between rotational channels gives the major contribution to the formation of a bound or a virtual state, and its influence on the electron wavefunction is substantial. The corresponding analysis based on the multichannel formula of Ross and Shaw, equation (15), leads to the following modification of equation (23):

$$\sigma_{fi} = \frac{ak}{k^2 + 2k \operatorname{Im} \kappa + |\kappa|^2}. \quad (24)$$

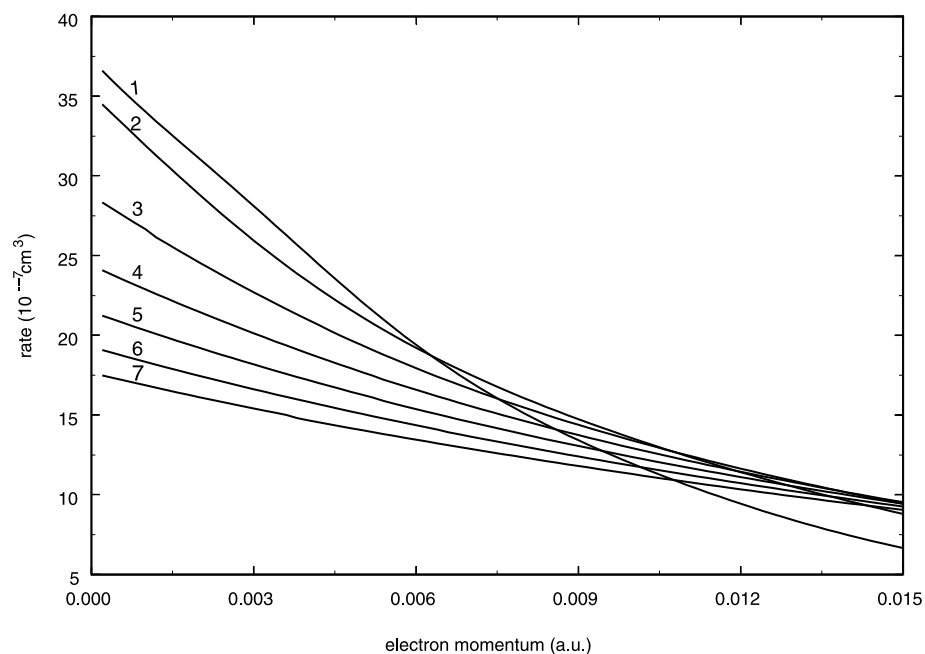


**Figure 2.** Rates for electron-impact rotational de-excitation of the HF molecules in different rotational states  $j$ .

The  $S$ -matrix pole acquires a non-zero real part. Constants  $\kappa$  and  $a$ , as well as the positions of  $S$ -matrix poles, depend on  $J$ . This dependence was calculated for HF (Fabrikant 1996). For higher  $J$ , the pole moves further away from the origin, and its influence on the threshold behaviour becomes weaker.

Experimentally, the influence of dipole-supported bound and virtual states was detected in studies (Frey *et al* 1994, 1995, Hill *et al* 1996) of rotational de-excitation of polar molecules by low-energy (Rydberg) electrons. The dependence on  $k$  of the rate constant,  $\mathcal{K} \propto k\sigma_{fi}$ , is an indication of deviation from the Wigner law and a signature of diffuse dipole-supported states. In figure 2, we present de-excitation rates for electron collisions with rotationally excited HF. By comparing this behaviour with the experimental data (Hill *et al* 1996), it was found that the energy of the  $\text{HF}^-$  virtual state at  $J = 0$  is about 1.3 meV.

**2.4.3. Symmetric-top molecules.** In symmetric-top molecules, rotation reduces the dipole moment, but does not average it to zero, as for diatomic and non-symmetric polyatomic molecules. The reduced dipole moment  $D_{\text{av}}$  can be defined as  $D_{\text{av}} = K/\sqrt{J(J+1)}$ , where  $J$  is the rotational angular momentum and  $K$  is its component about the symmetry axis.

For  $J = K = 0$ , the dipole moment is completely averaged out due to rotation. In addition, there is only one scattering channel at electron energies below the first rotational excitation threshold. Therefore, the threshold law in this case is the same as for a diatomic molecule. In particular, if the binding energy in the fixed-nuclei approximation is less than a tenth of the rotational constant, the bound state is transformed into a virtual state. If  $J > 0$  but  $K$  is still low, the molecular dipole moment is still averaged out (for  $K = 0$ ) or almost averaged out (for low  $K$ ). However, the initial scattering channel is rotationally coupled with other channels corresponding to scattering by states with lower rotational energies. As a result, the  $S$ -matrix

pole moves off the real axis in the complex energy plane but stays on the non-physical sheet (Fabrikant and Wilde 1999). The behaviour of the  $S$ -matrix element for a rotationally inelastic process is given by equation (22).

At higher  $K$ ,  $D_{av}$  grows and the  $S$ -matrix element for a rotationally inelastic process can be written, similarly to equation (22), as  $k^{\lambda+1/2} F(k^{2\lambda+1})$  (Fabrikant 1983), where  $F$  is a meromorphic function of its argument. The threshold exponent  $\lambda + \frac{1}{2}$  depends now on  $J$  and  $K$  (Engelking 1982). For calculation of the threshold exponent, the dipolar coupling between the degenerate channels (so-called strongly coupled channels) is important (Engelking 1982, Engelking and Herrick 1984). For a subcritical reduced dipole moment, the analogue of equation (22) has the form (Frey *et al* 1995)

$$\sigma_{fi} = \frac{ak^{\lambda+1/2}}{k^{2\lambda+1} + \kappa^{2\lambda+1}} \quad (25)$$

where  $\lambda$  is determined in the same way as in equations (17) and (18) but includes couplings only between degenerate channels. The effect of a non-zero averaged dipole moment is more important for oblate symmetric tops (such as  $\text{NH}_3$ ) whose rotational distribution at room temperature is dominated by states with  $K$  close to  $J$ . For prolate symmetric tops,  $K$  is typically small compared to  $J$ .

The most populated states at room temperature are those with  $K \ll J$ . They lead to the  $S$ -matrix behaviour in equation (22) with complex  $\kappa$ . The  $S$ -matrix poles in the energy plane at  $J > 0$  are similar to the virtual-state pole in the sense that they do not represent any quasibound states and are not associated with a time delay in scattering. Their imaginary part is positive, whereas it should be negative for quasibound states. However, they can substantially increase the near-threshold cross sections if their positions are close to the origin. Results of calculations for methyl chloride are discussed in Fabrikant and Wilde (1999).

### 2.5. Polarization and other dispersion potentials

Interactions among fragments of an atomic or molecular system are not, strictly speaking, short ranged. Two-body break-up processes, even when the fragments are uncharged, always involve multipole interactions that decrease with some reciprocal power of the distance between the fragments: examples include the detachment of an electron from a negative ion, governed at large distances by a  $1/r^4$  polarization potential, and the van der Waals ( $1/r^6$ ) interaction between neutral ground-state atoms of a dissociating diatomic molecule. The availability of new high-resolution photon sources for near-threshold spectroscopy, advances in the experimental observation of positron–atom collisions, the curious behaviours of ultracold gases, the continuing interest in the stability and detachment of new species of negative ions and the continued importance of low-energy electron propagation through molecular gases all require an improved understanding of the effects of these multipole interactions on two-body break-up processes.

Interaction potentials of the form  $-\beta/2r^s$  with  $s > 2$  are sometimes termed ‘short range’ because they are dominated by inertia (i.e. by the centrifugal barrier) at large distances. In this section, in contrast, we refer to these interactions as ‘dispersion forces’. The term ‘dispersion’ emphasizes that fragmenting systems interact via the exchange of virtual photons; the coefficients  $\beta$  calculated in standard references using dispersion relations (Marinescu *et al* 1994, Marinescu and Dalgarno 1995). *Dispersion forces modify the form of the effective range expansion*; even the leading term of the expansion (i.e. the threshold law) is changed for sufficiently high angular momentum states. This characteristic of dispersion forces, and their relevance to virtually all two-body break-up processes, warrants a careful elucidation of the required modifications of Wigner’s theory.

The role of dispersion forces in the scattering of slow particles was outlined by Landau and Lifshitz (1977, section 132) using Born's approximation. In particular, that reference shows (Landau and Lifshitz, section 132, problem 4) that dispersion forces produce a long-range (or 'anomalous') contribution to the phase shift of

$$\frac{\sqrt{\pi} m \beta}{4 \hbar^2} \frac{\Gamma((s-1)/2) \Gamma(\ell - (s-3)/2)}{\Gamma(s/2) \Gamma(\ell + (s+1)/2)} k^{s-2} \quad s > 3. \quad (26)$$

For sufficiently high  $\ell$ , this long-range phase shift will dominate the short-range shift that follows the Wigner law. Also, in the particular case of s-wave scattering from a  $1/r^3$  potential, the phase shift was found to vary as  $k \ln k$  near threshold.

Effective range expansions for dispersion potentials were obtained for  $s = 4$  using the Mathieu functions (O'Malley *et al* 1961, Holzwarth 1973) and for arbitrary  $s$  using the nonlinear first-order equation for the phase shift (Levy and Keller 1963). The latter method has been generalized to anisotropic potentials (O'Malley 1964, Fabrikant 1984). The two-potential formula of scattering theory can also be used to obtain effective range expansions (Hinckelman and Spruch 1971) even for the case of  $s = 3$  (Shakeshaft 1972).

Here, we will simply sketch a derivation of the threshold laws for dispersion forces, following closely the arguments presented in section 2.1. We begin with an analysis of the threshold wavefunctions, and deduce the threshold laws through an analysis of the scaling of Schrödinger's equation with energy. The presentation differs from that in section 2.2 largely because the phase shift is now defined relative to an *energy-dependent* phase  $[v - (\ell + \frac{1}{2})]\pi/2$  of waves in the combined dispersive and centrifugal potentials. This 'renormalization' of the centrifugal phase shift (i.e. the 'anomalous' phase described above) is the key to understanding threshold laws in dispersive potentials.

If short-range forces can be neglected beyond  $r_0$ , then Schrödinger's radial equation (in atomic units) for a reduced mass  $\mu$  and for  $r > r_0$  is

$$\left[ \frac{-1}{2\mu r^2} \frac{d}{dr} r^2 \frac{d}{dr} - \frac{\beta}{2r^s} + \frac{\ell(\ell+1)}{2\mu r^2} - E \right] R_\ell(r, E) = 0 \quad (27)$$

which now contains the dispersion potential  $V_s = -\beta/2r^s$  as well as the centrifugal barrier. There are now *four* readily identifiable regions of  $r$ : a core region ( $r < r_0$ ), a dispersion zone ( $r_0 < r < [\mu\beta/\ell(\ell+1)]^{1/(s-2)}$ ), an inertial zone ( $[\mu\beta/\ell(\ell+1)]^{1/(s-2)} < r < 1/\sqrt{2\mu E}$ ) and a far zone ( $r > 1/\sqrt{2\mu E}$ ). Note that the inertial zone is non-existent in the important case of s-wave scattering ( $\ell = 0$ ).

Solutions of equation (27) exactly at threshold ( $E = 0$ ) are Bessel functions of order  $\eta = 2\ell + 1/(s-2)$  and of a scaled variable  $x = [2/(s-2)]\sqrt{\mu\beta}/r^{s-2}$ . A pair of linearly independent solutions are simply

$$\begin{aligned} \sqrt{r} R_\ell^{(1)}(r > r_0, E = 0) &= J_\eta(x) \underset{r \rightarrow 0}{\sim} \sqrt{\frac{2}{\pi x}} \sin\left(x - \frac{1}{2}\pi\left(\eta - \frac{1}{2}\right)\right) \\ \sqrt{r} R_\ell^{(2)}(r > r_0, E = 0) &= Y_\eta(x) \underset{r \rightarrow 0}{\sim} -\sqrt{\frac{2}{\pi x}} \cos\left(x - \frac{1}{2}\pi\left(\eta - \frac{1}{2}\right)\right). \end{aligned} \quad (28)$$

Note that these solutions oscillate rapidly (for attractive dispersion potentials) near the origin, due to the unphysical singularity of the  $1/r^s$  potential. The second solution,  $Y_\eta$ , is indeterminate when  $\eta$  is an integer. In this case,  $Y$  is determined in standard texts by an application of l'Hospital's theorem, and its series expansion contains a logarithmic term in  $r$ . All partial waves of the  $1/r^3$  potential ( $s = 3$ ) of current interest in ultracold collisions have integral values of  $\eta$ . The logarithm complicates the analysis of threshold laws and the

effective range expansion. A rigorous mathematical proof of the threshold law for repulsive  $1/r^3$  interactions was given by Shakeshaft (1972) using the theory of Hinckelman and Spruch (1971) and later by Gao (1999) using a complete quantum defect theory. Here, we provide a more elementary derivation of the threshold law based on the principles utilized in section 2.1 for short-range potentials.

The threshold wavefunction outside of the core boundary  $r_0$  is a superposition of the base pair in equation (28), described by a core phase shift  $\delta_0$  that varies with energy only on the scale of  $1/\mu r_0^2$  and can be considered constant,

$$\sqrt{r} R_\ell(r > r_0, E = 0) = \cos \delta_0 J_\eta(x) - \sin \delta_0 Y_\eta(x). \quad (29)$$

The leading terms of this threshold wavefunction *in the inertial zone* are obtained by retaining only the leading powers of  $x$  in the expansion of the Bessel functions

$$R_\ell(r, E = 0) \underset{r \rightarrow \infty}{\sim} \frac{\sin \delta_0 \Gamma(1 + \eta)}{\pi \eta C^\eta} \left[ r^\ell + \frac{\pi \eta C^{2\eta}}{\Gamma^2(1 + \eta) \sin(\delta_0)} \frac{F_\eta(r, C)}{r^{\ell+1}} \right] \quad (30)$$

where  $C = \sqrt{\mu\beta}/(s - 2)$  and

$$F_\eta(r, C) = \begin{cases} \sin(\pi\eta + \delta_0) / \sin \pi\eta & \eta \neq 1, 2, \dots \\ \frac{-2 \sin \delta_0}{\pi} \ln\left(\frac{C}{r^{(s-2)/2}}\right) + \cos \delta_0 + \frac{\sin \delta_0}{\pi} (\psi(1) - \psi(n-1)) & \eta = n = 1, 2, \dots \end{cases} \quad (31)$$

This form of the threshold wavefunction, valid when the centrifugal barrier dominates the dispersion potential, is reminiscent of equation (6) of section 2.1. A logarithmic dependence on  $r$  for integral values of  $\eta$  appears explicitly in equation (31). Below, we join this form of the wavefunction onto finite-energy solutions valid in the inertial zone. (As described earlier, the far zone is removed to infinity at threshold.)

At a finite energy,  $E > 0$ , we rewrite equation (27) in terms of  $z = kr$ , and  $M_\ell = \sqrt{r} R_\ell$ ,

$$\left[ z \frac{d}{dz} z \frac{d}{dz} + z^2 - \left(\ell + \frac{1}{2}\right)^2 \right] M_\ell(z, \mu\beta k^{s-2}) = -\frac{\mu\beta k^{s-2}}{z^{s-2}} M_\ell(z, \mu\beta k^{s-2}). \quad (32)$$

In contrast to Wigner theory, Schrödinger's equation is no longer homogeneous in  $z = kr$ , but depends as well on the scaled dispersion coefficient  $\mu\beta k^{s-2}$ . The threshold wavefunction equation (30) is readily cast in terms of this parameter, yielding

$$\sqrt{r} R_\ell(r, E = 0) \underset{r \rightarrow \infty}{\sim} \frac{\sin \delta_0 \Gamma(1 + \eta)}{\pi \eta (C')^\eta} \left[ z^{\ell+1/2} + \frac{\pi \eta (C')^{2\eta}}{\Gamma^2(1 + \eta) \sin(\delta_0)} \frac{F_\eta(z, C')}{z^{\ell+1/2}} \right] \quad (33)$$

where  $C' = \sqrt{\mu\beta k^{s-2}}/(s - 2)$ .

The right-hand side of equation (32) represents the dispersion potential. Neglecting it results in a Bessel function solution representing free propagation of the wave throughout the inertial and far zones. The right-hand side *must be incorporated, at least perturbatively*, for a smooth matching onto the threshold wavefunction in the inertial zone. This remark identifies  $\mu\beta k^{s-2}$  as the key perturbation parameter determining the threshold law and higher-order terms in this expansion provide the required modifications of the effective range expansion. The same conclusion emerges in the JWKB treatment of section 2.6.

2.5.1. *Even power-law potentials.* Perturbative solutions of equation (32) for even values of  $s$  were constructed by Cavagnero (1994), where it was noted that  $J_{\pm(\ell+1/2)}$  are *not* valid zeroth-order solutions. This surprising result stems from the fact that dispersion potentials are *secular perturbations* that drive the unperturbed system at resonance, leading to divergent solutions. Convergent solutions are obtained by shifting (or renormalizing) the angular momentum quantum number

$$(\ell + \frac{1}{2})^2 = \nu^2 + (\mu\beta k^{s-2})\Gamma^{(1)} + (\mu\beta k^{s-2})^2\Gamma^{(2)} + \dots \quad (34)$$

and adjusting the  $\Gamma$ 's precisely to avoid resonance. Correct zeroth-order solutions, valid as  $k \rightarrow 0$  throughout the inertial and far zones, are then simply

$$M_\ell^\pm(z, \mu\beta k^{s-2}) = J_{\pm\nu}(z) + O(\mu\beta k^{s-2}). \quad (35)$$

Solving equation (34) for  $\nu$  yields

$$\nu = (\ell + \frac{1}{2}) + \text{constant} (\mu\beta k^{s-2}) + \dots \quad (36)$$

Within the inertial zone, equation (35) then has the form

$$M_\ell^\pm(z) \sim z^{\pm\nu} = z^{\pm(\ell+1/2)} (1 \pm a\mu\beta k^{s-2} \ln z + \dots) \quad (37)$$

for which only the first factor enters near threshold. The finite-energy wavefunction resulting from the continuation of equation (33) then has the limiting form

$$\sqrt{r}R_\ell(r, E) = (1/k^{\ell+1/2}) [J_\nu(z) + \text{constant} k^{2\ell+1} J_{-\nu}(z)] \quad (38)$$

reminiscent of Wigner's theory. However, within the far zone, the Bessel functions now have phases of  $-\nu\pi/2$  in place of  $-\ell\pi/2$ , with the result

$$\tan \delta \sim \text{constant} k^{s-2} + \text{constant} k^{2\ell+1} \quad s = 4, 6, 8, \dots \quad (39)$$

The first term arises from the long-range phase shift associated with  $\nu$ , and the constant in front of it agrees precisely with the Born result, equation (26). For  $2\ell + 1 < s - 2$  the Wigner threshold law is preserved, while for higher  $\ell$  the dispersion potential dominates. This result is also in accord with the early proof (Spruch *et al* 1960) for the polarization potential, and with the general remarks of Rau (1984a).

The wavefunction in equation (38) holds throughout the inertial and far zones, but is normalized at the origin; its small  $r$  form is simply the energy-independent equation (29). Accordingly, the amplitude in equation (38) diverges at threshold as  $k^{-(\ell+1/2)}$ . Normalization of this wavefunction per unit energy then requires multiplication of both equations (29) and (38) by  $k^{\ell+1/2}$ . This amplitude factor at small  $r$  indicates that *inelastic processes* are still governed by the Wigner law, independent of the dispersion potential; see also section 2.6 below.

2.5.2. *Odd power-law potentials.* The secular perturbation theory (Cavagnero 1994, Rosenberg 1998) no longer suffices to determine the leading term in the expansion of  $\nu$  when  $s$  is odd. This stems from the fact that the dispersion potential couples  $J_{\ell+1/2}$  and  $J_{-\ell-1/2}$  directly in some order, both of which are solutions of the unperturbed equation. An alternative procedure, adopted below, is to write down a formally exact solution of equation (32) in terms of a Laurent series (Spruch *et al* 1960, Peach 1979, Gao 1999), and to evaluate  $\nu$  from the expansion of an infinite determinant in powers of  $\mu\beta k^{s-2}$ . A similar expansion is considered below in section 2.6.

For odd power-law potentials ( $s = \text{odd}$ ), but with  $\eta$  non-integral, the result is

$$\nu = (\ell + \frac{1}{2}) + \text{constant} (\mu\beta k^{s-2}) + \dots \quad (40)$$

The remainder of the derivation proceeds as above, with the result

$$\tan \delta \sim \text{constant } k^{(s-2)} + \text{constant } k^{2\ell+1} \quad s = 5, 7, 9, \dots \quad 2\ell \neq s - 3, 3s - 7, \dots \quad (41)$$

precisely as with  $s$  even.

Turning now to the case of integral  $\eta$ , equation (31) demonstrates that for fixed  $z$ ,

$$F_\eta(z, C') \rightarrow \frac{(s-2) \cos(\delta_0)}{\pi} \ln k \quad (42)$$

so that the near-threshold wavefunction has the form

$$\sqrt{r} R_\ell(r, E) = (1/k^{\ell+1/2}) [J_\nu(z) + \text{constant } k^{2\ell+1} \ln k J_{-\nu}(z)]. \quad (43)$$

For the important case of s-wave scattering in a  $1/r^3$  potential (see the excellent review by Weiner *et al* 1999, section 4), one finds

$$\nu = \frac{1}{2} + \mu\beta k \quad s = 3 \quad l = 0. \quad (44)$$

The long-range phase shift associated with this potential is accordingly linear in  $k$  and is dominated by the  $k \ln k$  term in equation (43). Accordingly, as in the Born theory,

$$\tan \delta = \text{constant } k \ln k \quad (45)$$

a result surmised in Levy and Keller (1963) and first proved by Shakeshaft (1972). The elastic scattering cross section from a  $1/r^3$  potential thus diverges at threshold as  $(\ln k)^2$ .

While no general derivation of the threshold laws for other integral values of  $\eta$  has yet been presented, the procedure just outlined should be adequate to construct the relevant threshold behaviours. This analysis demonstrates that, while dispersive potentials are ‘shorter ranged’ than the centrifugal barrier, they nevertheless modify the Wigner threshold law for most partial waves, and in the case of the  $1/r^3$  potential, can even lead to divergent cross sections.

Finally, it is interesting to compare the above analysis to that for the Coulomb potential. Setting  $s = 1$  in equation (32) shows that the Coulomb potential cannot be treated perturbatively except at very small distances. The relevant perturbation theory is then performed, not in terms of  $z$ , but in terms of the parameter  $x \sim \sqrt{r}$ . The reason for the difference lies in the fact that the dispersion zone lies inside the inertial zone, while the Coulomb zone lies outside it.

## 2.6. JWKB treatment

In many cases, the feature already mentioned at the beginning of section 2, that the threshold behaviour arises from large  $r$  where the local wavenumber is slowly varying, permits a simpler JWKB treatment that is sufficiently accurate to forgo a complete MQDT analysis of the base functions ( $f, g$ ) of the respective long-range potential. Figure 3 is instructive in the insight it provides into the relevant MQDT parameters. At an energy  $E > 0$ , the propagation from small  $r$  in the vicinity of the reaction zone to infinity involves two phase integrals, from  $r_0$  to  $r_1$  and from  $r_1$  to  $\infty$ , where  $r_1$  is the classical turning point.

In the usual way of a Langer (1937) modification,  $\ell(\ell + 1) \rightarrow \bar{\ell}^2$ , with  $\bar{\ell} = \ell + \frac{1}{2}$  for a JWKB treatment, we have  $r_1 = \bar{\ell}/k$ . The tunnelling integral in this treatment is precisely the first MQDT parameter,

$$\mathcal{B}^{1/2} = (2\pi\bar{\ell})^{1/2} \exp \left[ - \lim_{r \rightarrow 0} \left( \int_r^{r_1} |k(r')| dr' + \bar{\ell} \ln r \right) \right] \quad (46)$$

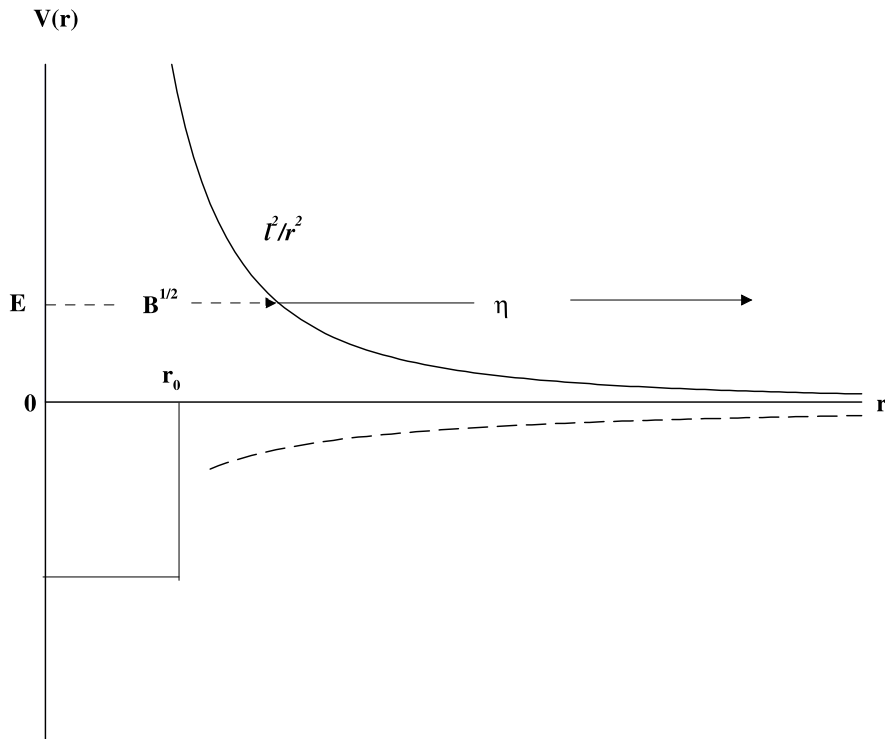


**Figure 3.** Schematic of MQDT parameters  $B$  and  $\eta$  as JWKB phase integrals at an energy  $E$ . A short-range potential, the angular momentum barrier and an attractive dispersion potential (long-broken curve) are shown.

where  $k(r)^2 = k^2 - \bar{\ell}^2/r^2 - 2V_s(r)$  is the local wavenumber. Note that for a short-range potential,  $|k(r')|$  in equation (46) reduces to  $\bar{\ell}/r$  and  $B^{1/2}$  to the  $k^{\bar{\ell}}$  of section 2.1.

Whereas the tunnelling phase integral modifies the amplitude of the radial wavefunction, in addition, there is a real phase stemming from the region  $r_1$  to infinity arising from the angular momentum potential and any other  $V_s(r)$  such as a power-law dispersion potential indicated in figure 3. This defines a ‘long-range phase shift’

$$\delta_\ell = (\pi/4) + \lim_{r \rightarrow \infty} \left[ \int_{r_1}^r k(r') \, dr' - kr + (Z/k) \ln r \right]. \tag{47}$$

The definition includes the usual  $\pi/4$  contribution from the turning point and a logarithmic contribution when there is a Coulomb potential. When equation (46) has only the angular momentum potential,  $\delta_\ell$  reduces to the  $-\pi \ell/2$  contained in the asymptotic behaviour of  $(f, g)$ .

Besides providing these JWKB interpretations of the MQDT parameters, figure 3 also clarifies the different effects that a power-law potential  $V_s(r) = -r^{-s}$  has on the two results in equation (5) as noted in our discussion of dispersion forces in section 2.5. For an inelastic process, the outgoing wavefunction in that channel has perforce to tunnel out from  $r_0$  through the angular momentum barrier as the bodies separate to infinity, the ‘initial feed’ at  $r_0$  having resulted from some other incoming channel (for which  $k$  in the outgoing channel of interest is not a significant parameter). This tunnelling induces the  $k^{2\ell+1}$  behaviour (which may be valid for only a tiny energy region above threshold (Slater *et al* 1978)), any other  $V_s(r)$  only contributing to further modulations of the outgoing wavefunction and thereby further

$k$  dependences. On the other hand, for elastic scattering, the bodies starting at  $r \rightarrow \infty$  need never tunnel in through the angular barrier all the way to  $r_0$  but only part way to be able to scatter from  $V_s(r)$  (Rau 1984a).

The JWKB results in equations (46) and (47) also provide quantitatively accurate  $\mathcal{B}$  and  $\delta_\ell$  for any power-law potential,  $V_s = -\beta/2r^s$ . The simple integrations involved in the two expressions can even be carried out analytically. Thus, for instance, for the polarization field  $s = 4$  of section 2.5, its contribution to  $\delta_\ell$  is

$$\delta_\ell = \int_{r_1}^{\infty} dr ([k^2 - (\bar{\ell}^2/r^2) + (\beta/r^4)]^{1/2} - [k^2 - (\bar{\ell}^2/r^2)]^{1/2}). \quad (48)$$

Expanding in powers of  $\beta$ , we have

$$\delta_\ell = (\beta/2) \int_{r_1}^{\infty} dr r^{-4} [k^2 - (\bar{\ell}^2/r^2)]^{1/2} - (\beta^2/8) \int_{r_1}^{\infty} dr r^{-8} [k^2 - (\bar{\ell}^2/r^2)]^{-3/2} + \dots$$

with  $r_1 = \bar{\ell}/k$ . By writing  $u = (k^2 r^2 / \bar{\ell}^2) - 1$ , each of these integrals reduces to a beta function,  $B(\frac{1}{2}, \frac{3}{2})$ , etc, so that

$$\delta_\ell = (\pi\beta k^2 / 8\bar{\ell}^3) + (15\pi\beta^2 k^4 / 128\bar{\ell}^7) + \dots \quad (49)$$

This result agrees with that of section 2.5 for large  $\ell$ , as expected for a semiclassical approximation. Note the expansion in terms of  $\beta k^{s-2}$ ,  $s = 4$ .

Remarkably, an obvious re-interpretation of powers of  $\bar{\ell}$  according to the prescription,  $8\bar{\ell}^3 \rightarrow (2\ell + 3)(2\ell + 1)(2\ell - 1)$ ,  $128\bar{\ell}^7 \rightarrow (2\ell + 7)(2\ell + 5) \dots (2\ell - 5)$ , that is,

$$\bar{\ell}^{p-1} \rightarrow \Gamma(\bar{\ell} + p/2) / \Gamma(\bar{\ell} + 1 - p/2) \quad (50)$$

makes equation (49) exact, valid also for small  $\ell$ . Quite generally, for arbitrary  $s$  and to arbitrary order  $n$  in powers of  $\beta$ , we obtain for the expression corresponding to equation (49)

$$\delta_\ell = \sum_{n=1} \frac{\sqrt{\pi} \beta^n}{4 n!} \frac{\Gamma(-\frac{1}{2} + \frac{1}{2}sn)}{\Gamma(1 - n + \frac{1}{2}sn)} \frac{\Gamma(\ell + \frac{3}{2} - \frac{1}{2}sn)}{\Gamma(\ell + \frac{1}{2} + \frac{1}{2}sn)} k^{n(s-2)}. \quad (51)$$

The leading term coincides with the results in equation (26). Similarly, the parameter  $\mathcal{B}$  can be evaluated from equation (46).

## 2.7. Ultracold collisions

The past two decades have witnessed the rapid development of technologies for lowering neutral atomic and molecular gases to temperatures well below 1 K. The relevant procedures—laser cooling, magnetic trapping, forced evaporative cooling, and buffer-gas cooling, to name a few—have produced samples as cold as tens of nanoKelvin, implying collision energies in the picoelectronvolt range. At these low energies, typically only a few partial waves contribute to scattering. Consider for example sodium, a commonly trapped alkali atom, whose p- and d-wave centrifugal barriers lie at energies  $E/k_B = 0.36$  and 5.3 mK, respectively. Its elastic cross sections at low temperatures are therefore strongly dominated by the first few partial waves.

Specifically, the threshold behaviour of colliding neutral atoms follows the rules outlined in sections 2.1, 2.5.1 and 2.5.2. The long-range interaction between neutral, ground state alkali atoms is dominated by an attractive van der Waals potential of the form  $-C_6/r^6$ . As a result, according to equation (39), elastic cross sections behave as  $\sigma_{\text{el}} \propto E^{2\ell}$  for  $\ell = 0$  or 1, whereas  $\sigma_{\text{el}} \propto E^3$  whenever  $\ell > 1$ . Thus only the s-wave cross section is non-vanishing at the lowest

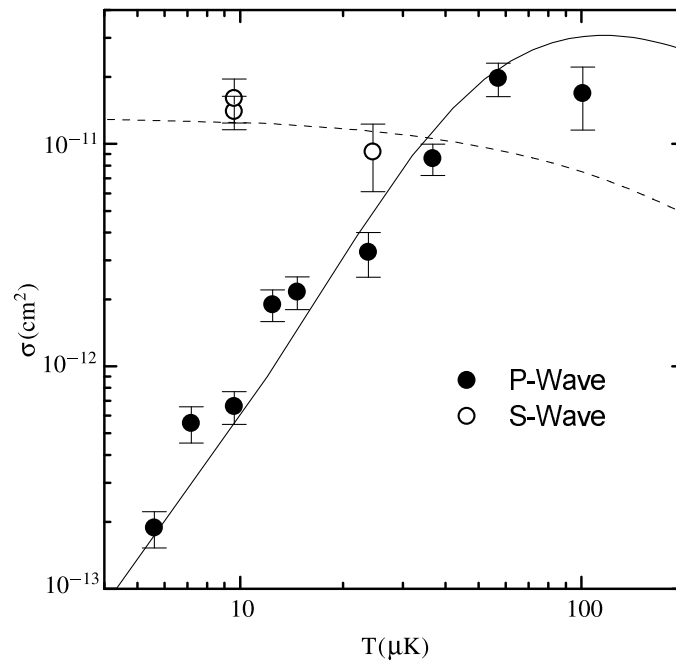


**Figure 4.** Low-energy elastic scattering cross sections for fermionic  $^{40}\text{K}$  atoms, illustrating the Wigner law in this system. When the atoms are spin-polarized (full circles) the Pauli exclusion principle forbids s-wave scattering, implying a  $T^2$  temperature dependence. In a gas with a mixture of spin states (broken curve), the familiar s-wave law is restored. (Adapted from DeMarco *et al* 1999.)

collision energies. Typically, higher partial waves exert little influence in ultracold-collision dynamics, except when shape resonances occur (Boesten *et al* 1997). Observation of these resonances often yields sensitive clues towards unravelling details of the interatomic potentials.

A notable exception to the dominance of s-wave collisions occurs in the scattering of *identical* fermionic atoms, i.e. atoms prepared in a single spin state by optical pumping (DeMarco *et al* 1999). In this case, identity of the spins of the two colliding atoms, combined with the Pauli exclusion principle, demands that the spatial component of the wavefunction have odd exchange symmetry, ruling out s-waves altogether. Figure 4 shows data illustrating this effect, based on a collisional re-thermalization measurement in  $^{40}\text{K}$ . The full circles exhibit the cross section for spin-polarized atoms, a circumstance which effectively ‘shuts off’ the s-wave component; a fit to the low-temperature data does indeed find the expected  $T^2$  dependence. In contrast, when the sample is not optically pumped, so that atoms in different spin states can collide, the s-wave cross section is restored (open circles).

Whereas threshold energy *dependences* of atomic cross sections have long been known, their *values* have only been accessible recently, in the context of cold-collision studies. Adequate knowledge of elastic cross sections is naturally important for assessing the prospects of evaporative cooling or buffer-gas cooling techniques that rely on high collision rates. In addition to energy-dependent cross sections, it is necessary to evaluate the s-wave scattering lengths  $a$ , which have been found to dominate the mean-field energy of Bose–Einstein condensates (Edwards and Burnett 1995). Indeed, for  $a < 0$ , it has long been known that an infinite, homogeneous Bose condensate is completely unstable against collapse (Huang and Yang 1957, Lee *et al* 1957). Confinement of these condensates in harmonic traps tends to

stabilize these systems, at least up to a certain critical number of atoms (Dodd *et al* 1996). Thus the microscopic threshold behaviour of each pair of atoms can control the macroscopic behaviour of the entire quantum gas.

Perhaps equally importantly, inelastic collision cross sections must also be assessed at low temperatures, particularly for magnetic trapping experiments. In a magnetic trap, paramagnetic atoms and molecules are confined by their  $-\vec{\mu} \cdot \vec{B}$  interaction with a spatially dependent magnetic field  $\vec{B}$ . If an inelastic collision process should flip the direction of the atom's spin, it is no longer trapped; too many of these collisions could bring a rapid end to the experiment. Moreover, spin-changing collisions often liberate an amount of energy corresponding to a fine- or hyperfine-splitting interval in the atom. These energies are typically far larger than the cloud temperature or even the trap depth, and can heat the atom cloud disastrously. For applications to evaporative or buffer gas cooling, it is essential that inelastic rates be significantly lower than elastic rates so that cooling can occur before all the atoms are lost. This requirement becomes ever more strict at lower temperatures, since exothermic s-wave cross sections diverge at threshold, in contrast to nearly constant elastic cross sections ( $k^{2\ell-1}$  versus  $k^{4\ell}$ , with  $\ell = 0$ ). On the other hand, inelastic collisions can occasionally prove beneficial. For example, current technologies for producing ultracold molecular samples tend to yield molecules in their high-lying vibrational and rotational states. Highly effective quenching of these modes is expected to assist in the production of ultracold ground state molecules (Balakrishnan *et al* 1998, Forrey *et al* 1998).

*2.7.1. Threshold scattering properties.* Apart from the simplest case of a pair of hydrogen atoms, cold-atom scattering lengths are virtually impossible to predict by purely *ab initio* means. Unless the interatomic potential energy surfaces are extremely accurately known, the errors accumulated in evaluating scattering phase shifts can become a significant fraction of  $\pi$ . Put another way, even those potentials determined by vibrational spectroscopy and high-energy scattering are optimized to different energy ranges than near threshold (Dulieu *et al* 1994).

Nevertheless, some general conclusions can be drawn even in the absence of specific information. Gribakin and Flambaum (1993) and Flambaum *et al* (1999) have approached the problem of scattering lengths and effective ranges for general  $-C_6/r^6$  potentials, within a semiclassical framework. Their main conclusion is the statistical statement, that the 'most likely' scattering length for a given  $C_6$  and reduced mass  $\mu$  is given by

$$\bar{a} = \frac{\Gamma(\frac{3}{4})}{\sqrt{2}\Gamma(\frac{5}{4})} \left( \frac{\sqrt{2\mu C_6}}{\hbar} \right)^{1/2}. \quad (52)$$

Moreover, they conclude that, on average, atomic scattering lengths are three times as likely to be positive as negative. Interestingly, the measured singlet and triplet scattering lengths of the alkali atoms do show a preference for  $a > 0$  (Weiner *et al* 1999), with 11 positive and five negative scattering lengths (this is admittedly a small sample size).

Burke *et al* (1998) refined this prediction within an exact quantum mechanical treatment cast in terms of quantum defect theory. Their result asserts that

$$a = -\bar{a} \tan \pi \mu [1 + \mathcal{G}(0) \tan \pi \mu]^{-1} \quad (53)$$

in terms of the zero-energy MQDT normalization parameter  $\mathcal{G}(0)$  and the quantum defect  $\mu$ . The value of  $\mathcal{G}(0)$  is within a few per cent of  $-1$  for virtually all atoms. Thus, treating  $\mu$  as a random variable distributed uniformly between  $-0.5$  and  $+0.5$ , equation (53) also predicts that approximately  $\frac{3}{4}$  of all scattering lengths are positive.

For more definitive information, we rely on experiments, which can determine scattering lengths in a variety of ways. In a few cases, direct collisional measurements of cross

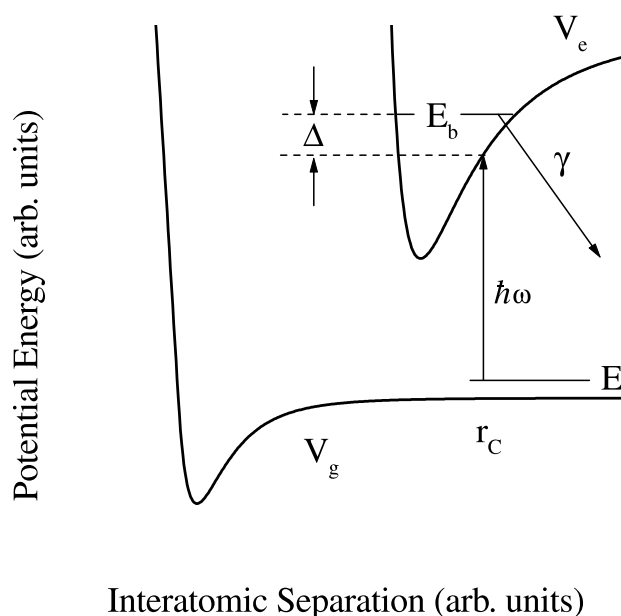


**Figure 5.** Schematic molecular potential curves illustrating the photoassociation process in ultracold atomic collisions. See text for details. (Adapted from Bohn and Julienne 1999.)

sections have been inferred by measuring thermalization rates (DeMarco *et al* 1999, Newbury *et al* 1995). However, the working tool for unravelling scattering lengths these days is photoassociation (PA) spectroscopy. This technique, first envisioned by Thorsheim *et al* (1987), is illustrated schematically in figure 5. The colliding atoms approach one another, governed by their ground state interaction potential  $V_g(r)$  (which may actually stand for a coupled-channel ground state). The collision takes place in the presence of a CW laser field detuned to the red of the atomic resonance by typically tens or hundreds of GHz. The atoms can then make a transition jointly into a bound state of the electronically excited potential  $V_e(r)$ . This level may then spontaneously emit a photon, or may be probed via a second laser. In any event, resonance with the bound state generally reveals itself through a diminished population of trapped atoms.

Quantitatively unravelling PA spectroscopy requires some understanding of the resulting lineshapes, which possess characteristic features arising from threshold effects. The basic lineshape, proposed by Napolitano *et al* (1994) and expanded by Bohn and Julienne (1999), is given by the thermal average of the loss rate constant  $(\pi\hbar/\mu k)|S_{\text{in,loss}}|^2$ , where  $|S_{\text{in,loss}}|^2$  is the squared scattering matrix element representing the transition from the incident channel to the loss channel. Here we consider only the s-wave contribution to this scattering. The scattering probability itself has formally a Breit–Wigner lineshape versus energy

$$|S_{\text{in,loss}}|^2 = \frac{\gamma\Gamma}{[E - (\Delta + E_0)]^2 + ((\gamma + \Gamma)/2)^2}. \quad (54)$$

Here  $\gamma$  is the spontaneous emission rate from the excited state,  $\Delta$  is the laser's detuning from this state, and  $\Gamma$  and  $E_0$  are the laser-induced stimulated rate and line shift, respectively.

Thus the relative strengths of these PA signals are governed primarily by the rate  $\Gamma$ , which is in turn proportional to the Franck–Condon overlap integral of the continuum and bound states. Indeed, exploiting the fact that PA transitions occur at fairly large values of  $r$

(e.g. tens of atomic units for typical detunings), Julienne (1996) has shown that a reflection approximation adequately represents the relative line strengths

$$\Gamma = IC_{\text{ex}}|f_{\text{g}}(r_{\text{C}})|^2. \quad (55)$$

Here  $I$  stands for the laser's intensity,  $C_{\text{ex}}$  for a factor that depends both on the excited state potential  $V_{\text{e}}$  and on the electric dipole transition operator and  $f_{\text{g}}$  is the energy-normalized continuum wavefunction in the electronic ground state. In this expression  $f_{\text{g}}$  is evaluated at the detuning-dependent 'Condon radius'  $r_{\text{C}}$ , which is the value of  $r$  at which the laser photon's energy just makes up the energy difference between  $V_{\text{g}}$  and  $V_{\text{e}}$ . Thus the photoassociation signal provides a fairly direct mapping of the ground state wavefunction at low collision energies, providing in turn scattering length information. Measurements of lithium scattering lengths have been performed in this way (Abraham *et al* 1996). In favourable cases of positive scattering length, the ground state wavefunction has the form  $f_{\text{g}} \propto \sqrt{k}(r-a)$ . If the experiment can probe values of the Condon radius comparable to  $a$ , then the PA signal at the corresponding detuning will possess a minimum, making an almost direct measurement of  $a$ . An analogous p-wave minimum was indeed useful in determining sodium scattering lengths (Tiesinga *et al* 1996).

Further refinements of PA spectroscopy extend these basic notions to multichannel wavefunctions and to rotationally resolved spectra. In this way, the sodium (Tiesinga *et al* 1996) and potassium (Burke *et al* 1999, Williams *et al* 1999) scattering lengths have been determined. Finally, the most definitive experiments are generally those that employ a second PA laser to drive a resonant transition from the first bound state to a bound state of the ground state potential lying below the incident thresholds. Thus the positions of the highest-lying bound states of the incident potentials can be measured. This information on energies just below the threshold is generally sufficient for extracting scattering lengths and other pertinent information just above threshold, reinforcing the connection between bound and continuum states in this energy range. Such measurements have proven valuable in lithium (Abraham *et al* 1997) and rubidium (Tsai *et al* 1997).

Even though the formal expression for scattering probability equation (54) has a Breit-Wigner form, its actual energy dependence near threshold is strongly shaped by the energy dependences of  $\Gamma$  and  $E_0$ . For example, given the  $k^{1/2}$  energy dependence of the energy-normalized ground state wavefunction  $f_{\text{g}}$ , equation (55) implies that  $\Gamma \propto \sqrt{E}$  near threshold, and of course vanishes altogether for  $E < 0$ . Upon thermal averaging, this shape results in a characteristic asymmetry in the lineshape, exemplified by a long tail to the low-frequency (red) side of the line (Napolitano *et al* 1994).

We note finally that scattering lengths are occasionally determined 'by accident.' An experiment by Myatt *et al* (1997) demonstrated that two spin states of  $^{87}\text{Rb}$  could be magnetically trapped simultaneously, even though it was expected that spin-changing collisions between the two would rapidly deplete the trap. The anomalously low spin-exchange rates were quickly understood to originate in the near equality (modulo  $\pi$ ) of the singlet and triplet phase shifts for this isotope (Kokkelmans *et al* 1997, Julienne *et al* 1997, Burke *et al* 1997). Since the triplet scattering length had already been determined by photoassociation, this happy accident provided the first determination of the Rb singlet scattering length.

**2.7.2. Manipulating threshold behaviour.** A remarkable feature that has emerged in ultracold-atom technology is the ability to tune threshold behaviour with external fields. This ability is tied to the fact that typical collision time scales (say, microseconds) are far longer than those

of internal atomic motions, such as spin precession or photoabsorption. Thus an external field can alter the atoms during the collision, altering in turn the way they interact.

For this purpose, application of electric fields (Marinescu and You 1998), magnetic fields (Stwalley 1976, Tiesinga *et al* 1993), and lasers (Fedichev *et al* 1996b, Bohn and Julienne 1997) have all been suggested. Tuning of scattering lengths, while of basic interest to the study of threshold behaviour, also offers the prospect of creating 'designer superfluids', i.e. Bose condensates with an arbitrary mean-field interaction energy.

The most promising of these techniques, and the only one so far demonstrated, has involved magnetic fields; we will accordingly focus on this case. The basic idea is that a pair of atoms colliding in a given state of total spin may possess a Feshbach resonance below a threshold corresponding to a spin state of greater fine or hyperfine energy. The zero-field position of this resonance typically lies at an energy which is too high for the atoms to reach at low temperature. However, by applying a magnetic field it may be possible to lower the resonance to a position much nearer threshold, by Zeeman-shifting the thresholds. This resonance will influence the zero-energy phase shift, and hence the scattering length. In particular, if the resonance is made

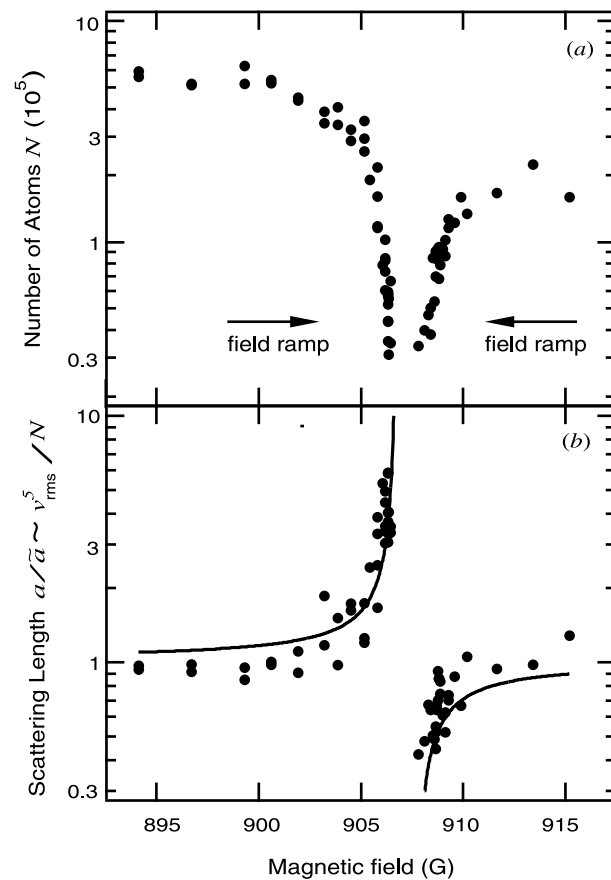


**Figure 6.** First observation of a magnetic-field-induced Feshbach resonance, in Bose-condensed  $^{23}\text{Na}$ . When the field reaches 907 G, the scattering length (shown in (b), normalized to its zero-field value) exhibits a characteristic resonance shape, implying tunability of the condensate's properties. (a) The effect of this resonance on survival probability of the condensed atoms is shown. Reprinted by permission from *Nature* **392** 151, copyright (1998) Macmillan Magazines Ltd.

to lie precisely at the incident threshold, the phase shift becomes  $\pi/2$ , and the usual  $\delta \propto k$  threshold behaviour of equation (5) is absent; the scattering length is then infinite. Thus such a resonance may be an appropriate tool for probing the Efimov phenomenon, as discussed in section 3.2.1. Artificially boosted cross sections may also be of use for evaporatively cooling species whose natural elastic cross sections may be too small. The isotopes  $^{85}\text{Rb}$  and  $^{39}\text{K}$  fall into this category, as do all spin-polarized fermionic atoms, which do not have s-wave cross sections at all.

Figure 6 presents the data from the first experiment to measure a magnetic-field-induced Feshbach resonance, in sodium (Inouye *et al* 1998). Subsequently, similar resonances have been observed in cold rubidium (Courteille *et al* 1998, Roberts *et al* 1998) and caesium (Vuletić *et al* 1999). The data shown in figure 6 were obtained in a Bose-condensed sample, whereby the scattering length itself is almost directly determined. (The mean-field contribution to the condensate's energy is proportional to  $a$ ; hence  $a$  can be extracted from the condensate's rate of expansion upon shutting off the trapping potential.) These resonances are extremely sensitive probes of interatomic potentials. Indeed, by fitting the detailed lineshape for trap loss, Roberts *et al* (1998) have generated the most accurate rubidium potentials to date for use in cold-collision studies.

As always, inelastic processes are lurking, ready to disrupt the experiment. Particularly in the case of a narrow Feshbach resonance, the colliding atoms have a lengthy interaction time, implying that the spin-exchange process has plenty of time to produce untrapped spin states. Interestingly, the experiment depicted in figure 6 is immune to spin-exchange, but suffers perhaps a more insidious inelastic process. Namely, the rate for three-body recombination rises precipitously near the resonance. In this process, two atoms combine into a molecule, while a third atom carries away the molecular binding energy. Since the binding energy is generally also enormous compared to the trap depth, three-body recombination is a significant contributor to trap loss. The rates for this process are expected to scale as the fourth power of the scattering length, and so can become devastating near the resonance (Fedichev *et al* 1996a, Nielsen and Macek 1999, Esry *et al* 1999). More details are provided in section 3.2.2.

### 3. Three-body threshold laws

The Wigner threshold laws follow rather rigorously from first principles owing to the clean separation between an inner region  $r < r_0$  where the wave motion is complicated, but varies slowly with  $E$ , and an outer region where the motion is well represented by partial waves whose asymptotic forms are rigorously known. In contrast, for three or more particles, there is no such separation between an inner and an outer region, and the asymptotic forms are not rigorously known. This is particularly true for charged particles since exchange of energy and angular momentum through Coulomb interactions can occur even at large distances if the kinetic energy is small, as it must be at threshold. The break-up of an atom or molecule into three or more fragments thus differs qualitatively from the break-up into only two fragments. To recognize this difference we will refer to the break-up into three or more fragments as 'fragmentation'. It remains true, however, as in the case of two fragments, that  $E$  is a significant variable only for the particular channel of interest and only for asymptotic separations.

The threshold laws for fragmentation are the concern of this section. Because rigorous asymptotic forms for multiparticle wavefunctions are often not in hand, the theory of fragmentation threshold laws is necessarily more approximate than for two-body reactions. As a consequence, experimental information has played a critical role in the development of the correct laws for charged particle fragmentation. An extensive discussion of the experimental work, however, is beyond the scope of this review. Instead, we will concentrate

on the theoretical developments that have led to the now generally accepted threshold laws.

As with two-body channels, it is worth noting that the initial configuration leading to the final state of interest plays no role in the energy dependence. Thus, electron-impact ionization of hydrogen and photo-double-detachment of  $\text{H}^-$  both involve the common  $(\text{p} + \text{e}^- + \text{e}^-)$  final state and share the same threshold law. However, such alternative phenomena may, because of selection rules, involve alternative  $\ell_i$  or other long-range forces. In an  $N_{\text{p}}$ -body channel that does not involve any Coulomb potentials (more accurately, any potential longer in range than  $1/r^2$ ), the longest-range potential for a non-zero  $\ell_i$  being the corresponding angular momentum barrier, the matrix element  $\mathcal{M}$  in equation (3) picks up a factor  $k_i^{\ell_i}$  from the final state wavefunction and equation (4) is modified to

$$\sigma \propto E^{(N-2)/2 + \sum_i \ell_i}. \quad (56)$$

If, on the other hand, an attractive Coulomb potential exists for a channel  $i$ , the wavefunction acquires a  $k_i^{-1/2}$  factor, so that each such  $i$  contributes an  $E^{-1/2}$  dependence to  $\sigma$  through the matrix element. Thus, the threshold law appropriate to a three-body channel,  $A^+ + B^- + C$ , is  $\sigma \propto E^{3/2}$ .

### 3.1. Wannier threshold laws

Most important for atomic physics are fragmentation processes involving several charged particles. An exact wavefunction for such an assembly at low energies is not available even for asymptotic separations between the particles. Wannier (1953) formulated an elegant classical interpretation of low-energy collisions between charged particles. Although the essentials of his treatment have been reaffirmed by theory (Rau 1971, 1984b, Peterkop 1971, Read 1984a) and experiments (Cvejanovic and Read 1974, Lablanquie *et al* 1990, Donahue *et al* 1982), questions on the behaviour of the interaction below and above the threshold, the absolute cross section and the detailed dependence of the angular and energy distribution remain. In this section, we will focus mainly on theoretical developments since the last reviews (Rau 1984b, Read 1984b) of the field.

Wannier's example of two electrons escaping from a positive charge illustrates the basic problem. Different simple pictures/descriptions of the asymptotic final state argue for different normalizations and, thereby, for different threshold laws. If the electronic wavefunctions are treated as individual Coulomb waves, each will contribute a  $k_i^{-1/2}$  factor in the matrix element in equation (4), leading to a linear threshold law (Rudge and Seaton 1965),  $\sigma \propto E$ , whereas in the case when one electron completely screens off the other, the product of a Coulomb wave and a plane wave contributes one such factor and the cross section behaves as  $\sigma \propto E^{3/2}$ . An alternative view which takes into account the interaction of a charged particle with the induced dipole gives a linear threshold law which oscillates logarithmically with energy (Temkin 1982, 1984, Greene and Rau 1985). Clearly, successive approximations to the independent electron picture yield a variety of threshold laws. What is required is a theory of correlated motion of electrons in the field of a positively charged ion.

Wannier's classical theory conjectures that the dominant configuration for the electrons is one in which they depart in opposite directions, whilst maintaining equal distances from the ion. That the electrons stay on opposite sides of the nucleus is immediately plausible because of the mutual electrostatic repulsion between the two slow electrons. The latter conjecture, of approximately equal distances or, equivalently in classical terms, equal speeds, is significant and crucial. With  $E = E_1 + E_2$  vanishingly small, any departure from the energy equipartition

will only be magnified during the escape, resulting in one of the electrons, the slower one, falling back into a closed orbit around the nucleus and only the faster electron being ionized.

Wannier analysed the coupled Newtonian equations of motion for the two electrons in such a subset of configuration space and demonstrated two classes of trajectories, ‘converging’ and ‘diverging’. In the former, the evolution is toward the central equipartition configuration,  $E_1 = E_2 = \frac{1}{2}E$ , whereas in the latter it is away from it, as time increases. At any non-zero energy above threshold, the converging trajectories are a set of measure zero relative to the diverging ones so that the latter determine the threshold behaviour.

In mass-scaled Jacobi coordinates (Fedorov and Jensen 1993, Barnea and Novoselsky 1998)

$$r_j = \sqrt{\frac{M_j m_{j+1}}{M_{j+1}}} \left( r_{j+1} - \frac{1}{M_j} \sum_{i=1}^j m_i \rho_i \right) \quad j = 1, 2, \dots, N_p - 1 \quad (57)$$

where  $\rho_j$  and  $m_j$  are, respectively, the independent particle  $j$  coordinates and masses, and  $M_j = \sum_{i=1}^j m_i$  is the total mass of the system, the kinetic energy operator has the symmetric form  $-\frac{1}{2} \sum_{j=1}^{N_p-1} \nabla_j^2$ , and the total energy of the particles is given in terms of the relative wavevectors  $k_j$  by  $E = \frac{1}{2} \sum_{j=1}^{N_p-1} k_j^2$ .

It is desirable, and indeed necessary as demonstrated by Wannier (1953), to employ a collective description of the evolution of the charged particles in space, en route to fragmentation. One such coordinate system, naturally suited to the collective motion of charged and neutral particles (see also section 3.2.1) is the hyperspherical coordinates (Smith 1960, 1962, Macek 1968, Fano and Rau 1986, 1996, Lin 1995). The hyper-radius  $R$  in terms of the mass-scaled radial coordinates is

$$R = \sqrt{\sum_{j=1}^{(N_p-1)} r_j^2}. \quad (58)$$

When  $R$  is small, all particles are close together and this parameter is a natural generalization of the interparticle distance  $r$  of the Wigner theory. Alternatively, fragmentation corresponds to large  $R$ , with the proviso that all of the interparticle coordinates also become large. This is expressed by setting  $r_j = R \sin \varphi_j$  and requiring that  $\varphi_j$  remain non-zero as  $R \rightarrow \infty$ . Thus, we will use as our set of coordinates the hyper-radius  $R$  and a set of hyper-angles denoted by the unit vector  $\hat{\mathbf{R}}$  in  $N = 3N_p - 3$  dimensions.

*3.1.1. Rau–Peterkop analysis.* When a group of charged particles fragments at nearly zero total energy, they move out of an inner ‘reaction zone’, where the motion is unknown but changes only slowly with the total energy  $E$ , into a region where the potential energy  $V(\mathbf{R}) = C(\hat{\mathbf{R}})/R$  is much larger than the kinetic energy. In this region, called the ‘Coulomb zone’, the particles may exchange energy and angular momentum before moving into the region called the ‘far’ zone, where the potential energy is small compared with the kinetic energy so that energy exchanges effectively vanish. With the boundary between the Coulomb and the far zones moving outward as  $1/E$  as  $E \rightarrow 0$ , the threshold law is mainly determined by motion in the Coulomb zone.

A key point of Wannier’s analysis is that, classically, only very specific configurations allow slow charged particles to escape to infinite distances. Except for an overall rotation of the system, these configurations have all the particles at fixed hyperangles, so that only  $R$  changes. Any other configuration would allow slower particles to screen the faster ones producing an exchange of energy so that, at threshold, the slower particles must fall back into

bound states. This corresponds to excitation rather than fragmentation. Fragmentation thus corresponds to orbits that concentrate in regions of unstable equilibrium. These configurations play an essential role and are called the scaling configurations  $\hat{\mathbf{R}}_s$  since only the overall size of the system changes with time. They are saddle points of the potential surface  $C(\hat{\mathbf{R}})/R$  in the space of hyperangles.

Since these orbits are unstable, only those that are very close to the scaling configuration lead to fragmentation. At the border between the reaction and Coulomb zones, only those orbits that lie within a certain angular window, whose size depends upon the excess energy, can escape. At threshold, the window is a point in  $\hat{\mathbf{R}}$ -space, but expands at a certain rate as  $E$  increases. This rate of expansion is a power law,  $E^{\zeta_w}$ , where  $\zeta_w$  is the Wannier index. The fragmentation cross section is proportional to the rate of expansion of the escape window.

Rau (1971) and Peterkop (1971) sought a semiclassical, rather than a purely classical, formulation of Wannier's arguments. We will articulate these arguments employing the formulation of Kazansky and Ostrovsky (1992, 1994). Motion near the scaling configuration is represented by the radial JWKB wavefunction

$$F(R) = K(R)^{-1/2} \exp \left[ i \int^R K(R') dR' \right] \quad (59)$$

where  $K(R) = \sqrt{2(E - C(\hat{\mathbf{R}}_s)/R)}$  is the local momenta for orbits exactly at the scaling configuration. To allow for motion near the scaling configuration, the complete wavefunction is written as a product of  $F(R)$  and another function  $\phi(R, \hat{\mathbf{R}})$ . For motion near the scaling configuration,  $\phi$  varies slowly with  $R$ . Upon substituting the ansatz  $\psi(R, \hat{\mathbf{R}}) = F(R) \phi(R, \hat{\mathbf{R}})$  into the Schrödinger equation, neglecting small terms of order  $R^{-2}$ , and introducing a mock time  $d\tau = dR/[R^2 K(R)]$ , we obtain a time-dependent Schrödinger equation,

$$i \frac{\partial \phi}{\partial \tau} - (h_0(\hat{\mathbf{R}}) + R(\tau)[C(\hat{\mathbf{R}}) - C(\hat{\mathbf{R}}_s)]) \phi = 0 \quad (60)$$

where  $h_0(\hat{\mathbf{R}})$  derives from the hyperangular part of the kinetic energy operator. It is essentially the generalized angular momentum operator of Smith (1960, 1962).

The general solution of such equations is given in terms of Feynman's propagator. The time  $\tau_0$  corresponds to a hyper-radius  $R_0$  on the border between the reaction and the Coulomb zones. The propagator preserves wavefunction normalization so that the initial flux at  $R_0$  evolves to the final flux at infinite distances. Part of the flux populates bound states and part represents fragmentation. It would be necessary to solve equation (60) exactly to find the proportion of bound and continuum states. Some work has been done to find the propagator by numerical solution of equation (60), but further approximations (Kazansky *et al* 1997) are needed.

An alternative approach, consistent with the semiclassical treatment, is to treat motion in all the coordinates semiclassically, using van Vleck's (1923) semiclassical propagator and the classical orbits of the full system. Such an analysis for a collinear model of the helium atom, in which the interelectronic angle was set to  $180^\circ$ , found the probability for double escape to fit a power law with the Wannier exponent (Rost 1994). All possible orbits were considered, but it was confirmed that only orbits in the neighbourhood of the scaling configuration lead to fragmentation. It was found that motion near the scaling configuration determined the fragmentation cross section for energies at least 10 eV above the threshold. This was the first indication that the Wannier theory applied over an extended energy range, and may not be limited to a small region near threshold.

To extract an expression for the threshold law, it is necessary to identify a part of the wavefunction that corresponds to fragmentation only. This has been done by expanding both

$C(\hat{\mathbf{R}})$  and  $h_0(\hat{\mathbf{R}})$  in a power series around  $\hat{\mathbf{R}}_s$  and retaining only the constant and quadratic terms. The resulting Hamiltonian is just that for coupled oscillators, and a transformation to normal modes leads to the Schrödinger equation for uncoupled oscillators with time-dependent coupling constants. The solutions of such equations are known (Macek 1990, Jakubassa-Amundsen and Macek 1989), so that they can be employed to extract an approximate wavefunction for large  $\tau$ , or, equivalently, large  $R$ . In accordance with the usual results of scattering theory (Mott and Massey 1965), the coordinates  $\hat{\mathbf{R}}$  at large  $R$  go over to the directions of the wavevector  $\hat{\mathbf{K}}$ . With the energy normalization we have used in equation (59), the scattering amplitude is proportional to  $\phi(\tau, \hat{\mathbf{R}}) \rightarrow \phi(\tau, \hat{\mathbf{K}})$ ,  $R(\tau) \rightarrow \infty$ . It follows that the total fragmentation cross section is given by

$$\sigma \propto \lim_{R(\tau) \rightarrow \infty} \int |\phi(\tau, \hat{\mathbf{K}})|^2 d\hat{\mathbf{K}}. \quad (61)$$

At first glance, because the approximate propagator also preserves normalization, it appears that the right-hand side of equation (61) is equal to unity, incorrectly implying a constant fragmentation cross section, characteristic of two-body Coulomb threshold laws in  $N$  dimensions. To resolve the apparent discrepancy with the Wannier law, it is necessary to examine the approximate time-dependent Schrödinger equation more closely.

In terms of the normal modes, the Schrödinger equation has the form

$$i \frac{\partial \phi}{\partial \tau} - \left( -\frac{1}{2} \sum_j \frac{\partial^2}{\partial \xi_j^2} + R(\tau) \sum_j C_{1j} \xi_j^2 \right) \phi = 0 \quad (62)$$

where  $C_{1j}$  are the expansion coefficients of  $C(\hat{\mathbf{R}})$  in the normal-mode coordinates  $\xi_j$ . Although the angular coordinates are limited to finite ranges, it is assumed that the coordinates  $\xi_j$  take on all values between  $\pm\infty$ . The constants  $C_{1j}$  may be either positive or negative. If they are positive, the motion in the  $j$ 'th mode is stable and integration over the normal coordinates is effectively limited to regions near the scaling configuration. Motion in the stable normal modes makes no contribution to the threshold law owing to the preservation of the wavefunction normalization in those degrees of freedom.

If  $C_{1j}$  is negative, then the  $j$ 'th mode is unstable and the solution oscillates infinitely rapidly for large  $\xi_j$  so that integrations over the wavefunction are also effectively limited to the scaling configuration, but integrations over the magnitude of the wavefunction are not. In this case, large values of the normal coordinates correspond to physically inaccessible values of the angular coordinates. Because the wavefunction does not vanish in these unphysical regions, the integral in equation (61) cannot be extended over all values of  $\xi$ , so that this part of the propagator does not preserve the normalization of the wavefunction, and the integral over the angular coordinate  $\hat{\mathbf{K}}_j$  will not be unity.

To find the wavefunction at infinite distances, we need the propagator in the unstable coordinates  $\xi_j$ . A form adapted to the Wannier theory is given in Jakubassa-Amundsen and Macek (1989) and Macek (1990), namely

$$K(\tau, \xi_j; \tau_0, \xi'_j) = (2\pi\omega_{bj}(\tau, \tau_0))^{-1/2} \exp \left[ \frac{i\dot{\omega}_{bj}(\tau, \tau_0)\xi_j^2 - 2\xi_j\xi'_j + \omega_{aj}(\tau, \tau_0)\xi_j'^2}{2\omega_{bj}(\tau, \tau_0)} \right] \quad (63)$$

where the functions  $\omega_{aj}(\tau, \tau_0)$  and  $\omega_{bj}(\tau, \tau_0)$  are solutions of the classical equations

$$\ddot{\omega}(\tau, \tau_0) + R(\tau)2C_{1j}\omega(\tau, \tau_0) = 0 \quad (64)$$

with initial conditions  $\omega_{aj}(\tau, \tau_0) = 1$ ,  $\dot{\omega}_{aj}(\tau, \tau_0) = 0$ ,  $\omega_{bj}(\tau, \tau_0) = 0$ ,  $\dot{\omega}_{bj}(\tau, \tau_0) = 1$ .

It will be shown below that as  $R \rightarrow \infty$  and  $E \rightarrow 0$ , the ratio  $\omega_a/\omega_b$  approaches a constant, while  $1/\omega_b$  vanishes as some power of  $E$  in the limit as  $E \rightarrow 0$ . Because  $1/\omega_b$  goes to zero, we can expand the exponential  $\exp[i\xi_j \xi'_j/\omega_{bj}(R)]$  in powers of  $1/\omega_{bj}$  and retain the first non-vanishing term. Usually the first non-vanishing term will be the constant term so that

$$\phi \rightarrow 2\pi \omega_{bj}(\tau, \tau_0)^{-1/2} \exp\left[i \frac{\dot{\omega}_{bj}(\tau, \tau_0)}{2\omega_{bj}(\tau, \tau_0)} \xi_j^2\right] \int d\xi'_j \exp\left[i \frac{\omega_{aj}(\tau, \tau')}{2\omega_{bj}(\tau, \tau')} \xi_j'^2\right] \phi(\xi'_j). \quad (65)$$

The cross section then becomes proportional to  $\prod'_j (2\pi |\omega_{bj}(\tau, \tau_0)|)^{-1}$ ,  $R(\tau) \rightarrow \infty$ , where the primed sum runs only over indices  $j$  for which  $C_{1j} < 0$ .

The functions  $\omega_{a,b}(\tau, \tau_0)$  are known exactly, but in this review, we emphasize the solutions along the lines sketched in section 2.1, and employed by Rau (1971). Rau (1971) pointed out that the threshold laws may be extracted from the  $E = 0$  solutions. Since  $\tau(E = 0) = -2(2|C_0|R)^{-1/2}$ , it follows that the solutions to equation (64) have the form

$$\omega = AR^{v_j^+} + BR^{v_j^-} \quad (66)$$

where  $v_j^\pm = -\frac{1}{4} \pm \frac{1}{4}\sqrt{1 - 16C_{1j}/|C_0|}$ , and  $A$  and  $B$  are constants determined by the initial conditions. As  $R \rightarrow \infty$ , the first term in equation (66) dominates and  $w_{bj}$  goes as  $R^{v_j^+}$ . For non-zero values of energy,  $R$  should be replaced by the Wannier radius  $R_w = |C_0|/E$  asymptotically. This gives  $|1/w_{bj}| \rightarrow E^{v_j^+}$ . There will be one such factor for each normal coordinate with  $C_{1j} < 0$ , so that we obtain the generalized Wannier threshold law for charged particle fragmentation

$$\sigma \propto E^{\sum'_j v_j^+} \quad (67)$$

where the primed sum runs over the indices of all unstable normal modes. Here we have used that the distribution is independent of  $E$ , which holds since  $\omega_{aj}(\tau, \tau_0)/\omega_{bj}(\tau, \tau_0)$  becomes a constant as  $E \rightarrow 0$ .

For the special case of only two particles, there is only one unstable mode  $j = 1$  and we obtain the celebrated Wannier threshold index for two electrons and a positively charged ion with charge  $Z$ . In this case, one finds

$$C_0 = -\frac{4Z - 1}{\sqrt{2}} \quad C_{11} = -\frac{12Z - 1}{2\sqrt{2}} \quad v_1^+ = -\frac{1}{4} + \frac{1}{4}\sqrt{\frac{100Z - 9}{4Z - 1}}. \quad (68)$$

For  $Z = 1$ , one obtains  $v_1^+ = \zeta_w = 1.127$ , first calculated by Wannier (1953). The irrational exponent differs greatly from the simple rational ones for two-body threshold laws discussed in earlier sections. The dependence of the exponent on  $Z$  reflects an interplay between the nuclear attraction and the repulsion between the electrons. The exponent becomes unity in the limit  $Z \rightarrow \infty$ , in accordance with the earlier remark that the product of two Coulomb waves gives a linear threshold law. The excess of the exponent from unity should, therefore, be seen as the suppression of double escape due to the unstable motion away from the potential saddle.

This result was extended to other three-particle systems (Kuchiev and Ostrovsky 1998, Feagin 1984, Klar 1981) and to ions with  $Z > 1$ . For the general three-particle system with arbitrary masses and charges, it is necessary to solve a high-order algebraic equation for  $C_{1j}$  and  $C_0$ , but the form of the threshold law remains unchanged. For ionization of neutral atoms by positron impact, Klar (1981) found  $\zeta_w = 2.651$ . Feagin (1995) has also examined terms of the next order beyond the quadratic in the expansion around the scaling configuration, obtaining a cross section for an extended energy region above threshold, and corresponding energy and angular distributions of the escaping electrons; see also Rau (1976).

In the demonstration just given, the power law does not depend upon the initial function  $\phi(\tau, \hat{\mathbf{R}})$ . Exceptions to this statement do occur owing to symmetry constraints. If the initial function is an odd function of  $\xi'_j$ , then even terms in the expansion of the propagator vanish and the first odd term determines the threshold law. Then the cross section is proportional to  $1/|\omega_b|^3$  and the threshold exponent is  $3\nu_j^+$ . An example of this symmetry effect is seen in the threshold exponent for ionization of atomic hydrogen by electron impact when the final state has  $^3S$  symmetry. Here the triplet function is spatially antisymmetric and thus corresponds to a function with one node so that the threshold exponent is 3.381 rather than 1.127 (Feagin 1984).

The differing exponents for singlet and triplet states were investigated experimentally by Lubell and co-workers (Lubell *et al* 1977). They found that singlet and triplet total cross sections had identical Wannier exponents. It was later found (Greene and Rau 1982, 1983) that states with total angular momentum greater than zero were also populated at threshold, and that both singlet and triplet states of the higher total angular momenta obeyed a similar power law, with the exponent of  $\zeta_w = 1.127$ . The argument in the previous paragraph for a higher exponent applies only for spatial antisymmetry that leads to a node at the Wannier configuration in the unstable direction, that is, antisymmetry under purely radial interchange of the electrons. This occurs only for  $^3S$  and  $^1P^e$  symmetries, all others having a piece of the wavefunction that remains symmetric under this interchange even while being overall spatially antisymmetric (Greene and Rau 1982, 1983). In retrospect, the spin-asymmetry experiments were the first experimental demonstration of threshold fragmentation into states with  $L > 0$ . As will be discussed below, *ab initio* computations (Kato and Watanabe 1997) show that states with  $L \geq 4$  give non-negligible contributions to  $e^- + e^- + H^+$  fragmentation at threshold.

The threshold law has been extended to four-particle fragmentation (Klar and Schlecht 1976, Grujic 1981, Feagin and Filipczyk 1990, Kuchiev and Ostrovsky 1998),  $A^{+Z} + e^- + e^- + e^-$ , where there are two unstable normal modes, and also to five-particle breakup. Since the scaling configuration is highly symmetric, with three electrons at the vertices of an equilateral triangle, the two unstable normal modes are degenerate. All calculations agree on the Wannier threshold law, but this agreement was shown to be fortuitous (Kuchiev and Ostrovsky 1998). Poelstra *et al* (1994) and Feagin and Filipczyk (1990) employed a spurious phase space factor  $(N_p - 2)$  in place of the mode degeneracy number. The mode degeneracy for the unstable mode accidentally becomes  $N - 2$  for such highly symmetric systems. For systems of lower symmetry, this is not the case, and the discrepancy becomes apparent even in the value of the index.

Comparisons of the Wannier threshold law with experiment (Cvejanovic and Read 1974) generally confirm the predictions of Wannier (1953) in equation (67) for two-electron escape from the field of a positively charged ion. Not only the energy exponent but various other features of energy and angular correlations contained in the wavefunctions have been confirmed experimentally (Rau 1984b, Read 1984b, Lablanquie *et al* 1990). The power law has also been investigated for other systems such as  $e^+ + e^- + A^+$  and  $H^+ + H^- + H^+$ . In these cases, the data do not rule out the Wannier law. Comparison of experiment and theory is not definitive for these systems because of large uncertainties in the data in the vicinity of threshold. The Wannier threshold law is now generally accepted, although its range of validity is not known. It is surprisingly large for the highly symmetric system  $e^+ + e^- + A^+$ , but may be rather small in other cases.

**3.1.2. Multicrossing models.** The Wannier theory obtains a wavefunction at zero energy that is a part of the total wavefunction, namely the part that leads to fragmentation. Even

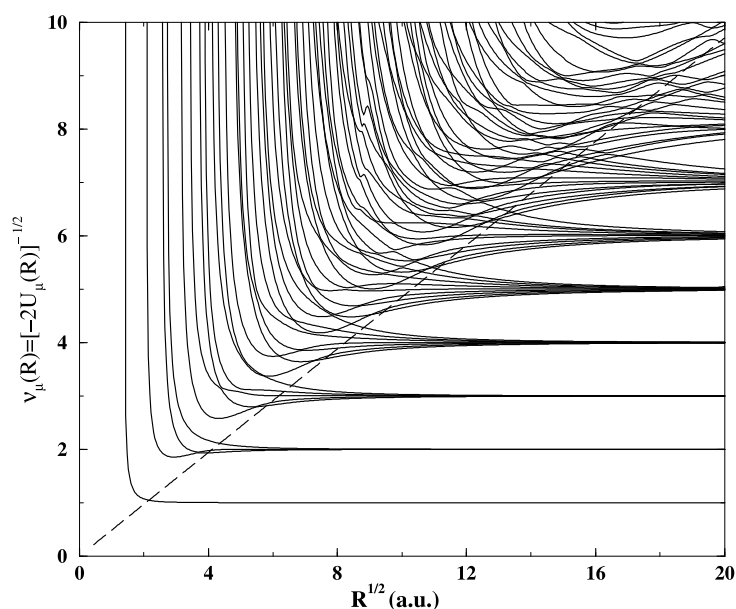


**Figure 7.** The adiabatic hyperspherical potential energy curves in  $\text{H}^-$  for the  $1\text{P}^0$  symmetry. The curves are shown on an effective quantum number scale,  $v_\mu(R) = [-2U_\mu(R)]^{-1/2}$ . The ridge line  $v_w = 18^{-1/4} R^{1/2}$  is shown as a broken line.

near the scaling configuration, there is also a part that does not represent fragmentation, but rather excitation into two-body channels. The propagator in equation (63) incorporates these channels, for example, through the eigenstates of the reduced Hamiltonian  $h(\hat{\mathbf{R}}) = h_0(\hat{\mathbf{R}}) + R[C(\hat{\mathbf{R}}) - C(\hat{\mathbf{R}}_s)]$ . The hyper-radius is a parameter in this Hamiltonian since the free-particle part refers only to the angular coordinates. The eigenstates and eigenvalues of  $h(\hat{\mathbf{R}})$  are the adiabatic eigenstates and eigenvalues,  $\phi_n(R; \hat{\mathbf{R}})$  and  $\varepsilon_n(R)R^2$ , introduced in connection with doubly excited states of two-electron species (Macek 1968).

A typical set of adiabatic hyperspherical potential energy curves are shown in figure 7. The curves are the eigenvalues  $\varepsilon_n(R)R^2$  as a function of the adiabatic parameter  $R$  and exhibit avoided crossings (Fano 1983). The width of the crossing region and the separation in energy at the avoided crossing are indicators of the strength of the coupling between the adiabatic potential energy curves. Transitions between different states occur at the avoided crossing regions. In the example of electron scattering from atoms, a useful picture of the ionization process emerges by considering multiple traversals of the adiabatic potential energy curves.

To locate these crossings, consider a plot of the potential taken along an unstable coordinate perpendicular to the line of the scaling trajectory. For two-electron species, there is only one unstable coordinate. The potential has the schematic shape shown in figure 8, with two Coulomb singularities at the edges and a barrier between them. The lowest eigenvalue  $\varepsilon_1(R)$  is located above the barrier for small  $R$ , at the top of the barrier for an intermediate value of  $R$ , and below the barrier for large  $R$ . For large  $R$ , the states are just the eigenstates of a one-electron atom, while for  $R \approx 0$  they are the hyperspherical harmonics (Erdelyi *et al* 1953) in six dimensions. At an intermediate value of  $R$ , the state sits right at the top of the barrier. At this value, the eigenstates concentrate in the potential valleys, and become Rydberg states. Higher energy curves retain the hyperspherical harmonic character so that the energy curve

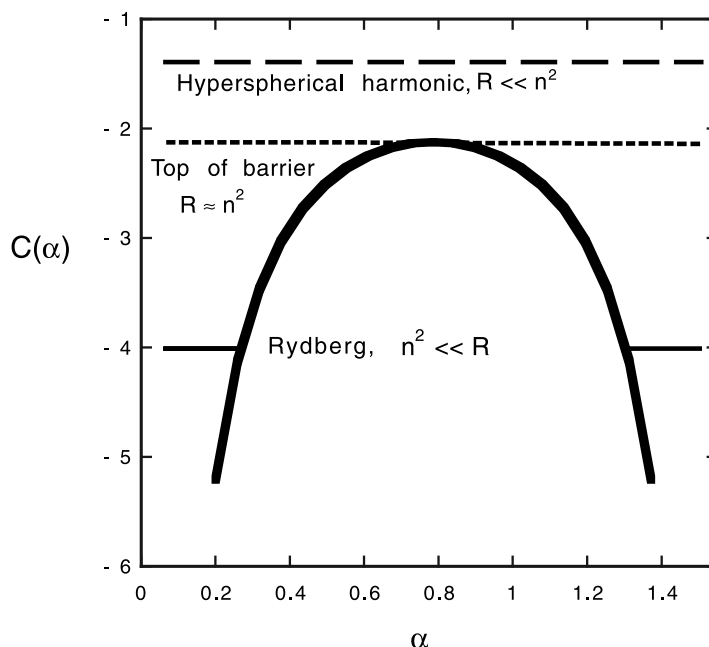


**Figure 8.** A schematic of top-of-the-barrier motion for two electrons is shown. Three eigenvalues typical of motion for small, intermediate and large  $R$  are displayed with long-broken, broken and full curves, respectively.

shows an avoided crossing where the lowest curve becomes Rydberg-like while the next higher curve still has the hyperspherical harmonic character. At still larger  $R$ , this state also comes down to the top of the barrier and undergoes a similar change to a Rydberg state. The process continues indefinitely, leading to a sequence of avoided crossings in the adiabatic potential curves.

Notice that the wavefunction at the top of the barrier sits at a position of classically unstable equilibrium on an inverted oscillator. The eigenstates in this top-of-barrier region are the adiabatic version of the eigenstates of the time-dependent Wannier propagator of equation (63). In effect, the eigenstates of the Wannier propagator are the diabatic states of  $h(\hat{R})$  in the region of the avoided crossing. The Wannier propagator follows the diabatic potential curve shown as a broken line in figure 7. At some radius of the order of  $R_W$ , the diabatic state represents ionization.

One such model of curve crossing has been proposed by Demkov and Osherov (1967). Using this model, it is possible to compute the probability for the system to remain in the bound two-body excited levels at a distance  $R$ , after a certain number of crossing regions have been traversed. If it is assumed that the diabatic state is effectively free for  $R \approx R_W$ , then the probability that the diabatic state survives the multiple crossings, which will be called the survival probability, equals the fragmentation probability. This probability should have the form given by the Wannier theory. For  $H^+ + e^- + H^+$ , the Wannier exponent is quite large, equal to 60.8. The multicrossing theory (Ovchinnikov 1990) obtained a numerical value close to this, but also found a  $\ln E$  term. It was later discovered that the  $\ln E$  came from an error in the potential curves, and should be removed. With this correction to the exponent, the multicrossing work agrees with the Wannier theory.

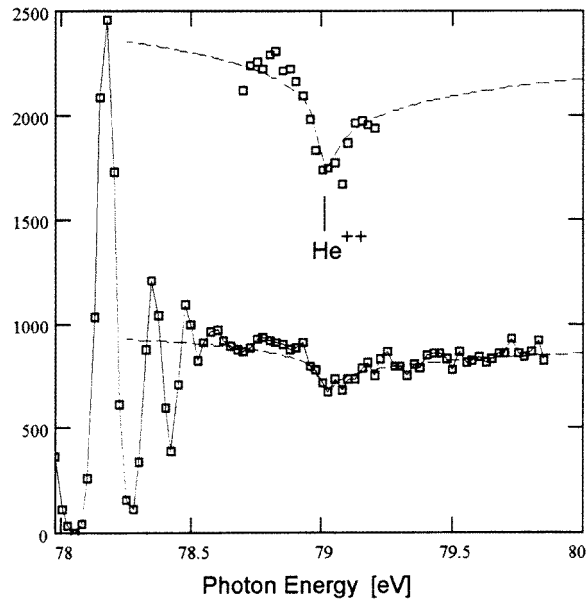


**Figure 9.** Photoelectron spectrum of helium near the double-ionization threshold. The broken curve is a Wannier law fit to data with differing amplitudes on either side of the threshold at 79 eV. Reprinted by permission from the authors, Cvejanovic *et al* (1995).

It can be concluded that multiple crossings of adiabatic energy curves is one way to construct a quantal version of the Wannier fragmentation theory. The multiple-crossing theory has the advantage that it gives a theory for the excitation of high-lying Rydberg states, and may even allow one to compute atomic processes for  $E < 0$ . In this connection, it has been pointed out (Fano 1974, Fano and Rau 1985) that the total cross section for excitation to all Rydberg states by electron impact should vanish as  $|E|^{1.127}$ , that is, the Wannier threshold law applies both above and below the fragmentation threshold. A quantitative treatment of this surmise is lacking but experiments (Buckman *et al* 1983, Cvejanovic *et al* 1996) bear out this conclusion (see figure 9).

The avoided crossings for  $e^- + e^- + H^+$  were computed for large values of  $R$  by Sadeghpour and Greene (1996). The transition probability at each avoided crossing was computed from a two-state linear Landau–Zener model. The probability  $\mathcal{P}(E)$  for making an infinite number of successive jumps, starting on the ground state of hydrogen, was written down as  $\mathcal{P}(E) = \mathcal{P}_{12}\mathcal{P}_{23}\mathcal{P}_{34} \dots = \exp(-2\pi S)$ , where

$$S = \sum_{n=1}^{\infty} \gamma_n = \sum_{n=1}^{\infty} \frac{\Delta_c^{(n)}}{8v_c^{(n)} P_c^{(n)}}. \quad (69)$$

$P_c^{(n)}$ ,  $v_c^{(n)}$  and  $\Delta_c^{(n)}$  are the values of the interchannel coupling between the adiabatic potential curves  $n$  and  $n + 1$ , the relative approach velocity along the curve  $n$ , and the separation of the curves  $n$  and  $n + 1$ , respectively. All of these parameters are evaluated at the hyper-radius of the closest approach, at the avoided crossing,  $R = R_c$ . Writing the relative velocity,  $v_c^{(n)} = \sqrt{2(E + C_0/R_c^{(n)})} = \sqrt{k^2 + c^2/n^2}$ , where  $R_c^{(n)} = (2C_0/c^2)n^2$  for the Rydberg electrons, it was found numerically that  $P_c^{(n)} = a/n$ , and  $\Delta_c^{(n)} = d/n^3$ , as expected on general grounds. The sum in equation (69) was evaluated by approximating it as an integral over a

continuous  $n$  to give in the limit as  $k \rightarrow 0$ , the absolute ionization probability

$$\mathcal{P}(E) = A_+ E^{\zeta_w} \quad E = 0^+ \quad (70)$$

where  $A_+ = (2c^2)^{-\zeta_w}$  and the Wannier exponent  $\zeta_w = \pi d/8ac$ . The sum in equation (69) can be analytically continued below the double-escape threshold for an arbitrarily large Rydberg state to yield

$$\mathcal{P}(E) = A_- |E|^{\zeta_w} \quad E = 0^- \quad (71)$$

where  $A_- = A_+ \{ [1 + (1 + 1/c^2)^{1/2}] / [1 + (1 - 1/c^2)^{1/2}] \}^{\zeta_w}$ . Two observations can readily be made: (a) the total probabilities for transitions below and above the double-escape threshold have similar dependences on energy and (b) the theory predicts an *asymmetric cusp* at  $E = 0$  ( $A_- > A_+$ ), consistent with the measurements of Cvejanovic *et al* (1996). Deviations from the power-law threshold are predicted to be exponential in  $\sqrt{E}$ , i.e.

$$\mathcal{P}(E) = A E^{\zeta_w} \exp(-Q\sqrt{E}). \quad (72)$$

Expanding the exponentials in half-integer powers of the energy gives a similar result as the numerical fit of Rost and Wintgen (1996) to the electron scattering data of Cvejanovic and Read (1974).

**3.1.3. Hidden-crossing method.** The multicrossing model is, in principle, an *ab initio* method since all of the ingredients of that theory are computationally accessible. Of course, the need to extract parameters for each avoided crossing from computed potential curves introduces uncontrollable errors since the fitting parameters depend upon the assumed functional form of the energy curves near the avoided crossings. An alternative, closely related, approach is based upon consideration of the asymptotic wavefunction in an adiabatic representation.

The asymptotic forms of radial wavefunctions are conventionally extracted by considering wavefunctions at complex  $R$ , i.e. on the circle at infinity. This idea was employed for the adiabatic representation of multiparticle wavefunctions. In the analytic continuation of the solutions to complex  $R$ , it was noted that the adiabatic functions themselves changed form dramatically. On the real axis, the adiabatic functions are known to represent atomic bound states. None of these functions correspond to positive energy as  $R \rightarrow \infty$ , so that the ionization components in the adiabatic representation are not seen explicitly. However, for complex values of  $R$ , the hydrogenic bound states change to harmonic oscillator states corresponding to waves concentrated on potential barriers. This happens because the top-of-barrier function  $\exp[ia_j \sqrt{R} \xi_j^2]$ ,  $a_j = \sqrt{|C_{1j}|}/2$  becomes exponentially decreasing for  $\text{Im } R > 0$ . The lowest eigenstate seeks out regions where the corresponding wavefunctions have minimum extent, and this is just at the top of the potential barrier where the classical motion is unstable.

The top-of-barrier eigenstates that appear at complex  $R$  are the fragmentation components missing on the real axis. One of the surprising results of this analysis is that the bound states only appear on a narrow strip along the real axis of  $R$ . Almost everywhere else on the unit circle at infinity, the adiabatic states are top-of-barrier harmonic oscillator states. It follows that fragmentation components can be extracted by analysing the adiabatic solutions for complex  $R$ . This has been done in Macek and Ovchinnikov (1996) but the analysis employs mathematical considerations that are relatively unfamiliar in atomic physics. Fortunately, the results are easily understood when the semiclassical approximation is used. One finds that the fragmentation component is given by

$$\Psi_{\text{frag}}(R, \hat{R}) \approx \frac{1}{\sqrt{K(R)}} \exp\left(i \int^R K(R') dR'\right) \phi(R; \hat{R}) \quad (73)$$

where  $K(R) = \sqrt{2(E - \varepsilon(R))}$ , and the integral goes along a path in the complex plane to a value  $R$  where the adiabatic function  $\phi(R; \hat{\mathbf{R}})$  corresponds to a top-of-barrier eigenstate. This function is analytically continued to real values of  $R$  to obtain the fragmentation amplitude

$$S(E) = S_0(E) \exp \left[ i \int_{R_0}^{\infty} (K(R) - K_0(R)) dR \right] \phi_{\text{asy}}(R_W; \hat{\mathbf{K}}) \quad (74)$$

where  $K_0(R) = \sqrt{2(E - C_0/R)}$ ,  $K(R) = \sqrt{2(E - \varepsilon_{\text{asy}}(R))}$ , and

$$\varepsilon_{\text{asy}}(R) = C_0/R - C_1/R^{3/2} - C_2/R^2. \quad (75)$$

$S_0(E)$  is a slowly varying function of the energy and  $R_0$  is a point on the real axis near the boundary of the reaction and Coulomb zones. The function  $\varepsilon_{\text{asy}}(R)$  represents an asymptotic expansion of the adiabatic eigenvalues for complex  $R$  on the circle at infinity. The wavefunction  $\phi_{\text{asy}}(R; \hat{\mathbf{R}})$  represents the corresponding asymptotic eigenfunction analytically continued to the real axis. It has the complex top-of-barrier form  $\exp[ia_j \sqrt{R} \xi_j^2]$ .

The threshold law emerges upon computing  $S(E)$  in the limit of small  $E$ . By expanding  $K(R)$  about  $K_0(R)$ , one finds  $\sigma \propto E^{\zeta_{\text{W}}^{\text{ad}}}$ , where the adiabatic Wannier index  $\zeta_{\text{W}}^{\text{ad}} = \sqrt{2 \text{Im } C_1^2 / |C_0| - \frac{1}{4}}$  differs slightly from the actual Wannier index  $\zeta_{\text{W}} = \sqrt{2 \text{Im } C_1^2 / |C_0| + \frac{1}{16} - \frac{1}{4}}$ . For  $Z = 1$ , the adiabatic index equals 1.104 instead of the correct value of 1.127. The difference between these two numbers is traced in the Rau–Peterkop analysis to a cross-term between  $R$  and the unstable motion, an explicitly non-adiabatic effect.

The slight error in the Wannier index is a disadvantage of the hidden-crossing theory. This is compensated by the fact that the theory gives an absolute cross section over an extended energy range. Comparison of the hidden-crossing theory with experiment shows that the theory is higher than experiment by about 10–20%. This is comparable to the results of Crothers (1986), although those results are limited to energies very near threshold.

In order to compute the fragmentation amplitude over an extended energy range, it was found necessary to include higher-order terms in the asymptotic expansion of  $\varepsilon(R)$ . These terms originate with the anharmonic terms in the expansion of  $C(\hat{\mathbf{R}}_{\text{rms}})$  near the scaling configuration. These give rise to the  $C_2/R^2$  term in equation (75), which in turn contributes an  $\exp(-Q\sqrt{E})$  factor in the cross section. This term is significant because it shows that higher-order terms in the cross section are not analytic in energy (see also section 3.1.2).

It turns out that the  $\sqrt{E}$  term has little effect on the cross section for fragmentation by electron impact because the anharmonic terms are small for potentials symmetric about the scaling configuration. For positron impact, the potential is not symmetric about the scaling configuration, and both cubic and quartic anharmonic terms contribute. The coefficient  $Q$  was computed in Ihra *et al* (1997) and found to equal 0.73. This is large enough to affect the cross section over an extended energy range. Measurements of the ionization of He by positron impact over an energy range from 0 to 10 eV were found to disagree with just the power-law expression  $AE^{\zeta_{\text{W}}}$  alone, but agreed with the extended law  $AE^{\zeta_{\text{W}}} \exp(-Q\sqrt{E})$ . The comparison with the data of Moxom *et al* (1996) essentially confirms the extended threshold law.

**3.1.4. *Ab initio* methods.** While the Wannier threshold law is now fairly well established, the present theory leaves many unanswered questions, e.g. the range of validity of the law, the value of the constant multiplying the power law, and some details of energy and angular distributions of the electrons. In addition, the extension of the theory to negative energies is not apparent. Some progress on these matters have been achieved by *ab initio* calculations.

The first *ab initio* calculations of the Wannier threshold cross section are those of Crothers and co-workers (Crothers 1986, Crothers and Lennon 1988). They computed the ionization amplitude for electron impact on helium using a product of a plane wave and an accurate bound target state wavefunction for the initial state and the modified Wannier functions of Rau (1971) and Peterkop (1971) for the final state. By extrapolating to  $E < 0$ , they were also able to obtain some information on doubly excited ‘ridge’ states (Loughan and Crothers 1997).

The time-dependent Schrödinger equation has been used recently (Pindzola and Robicieux 1998) to calculate the ionization cross section for electron scattering from a model helium atom. The ionization flux in the time domain was extracted by subtracting unity from the sum of the fragmentation flux for forming two-body ionic bound states. General agreement with the Wannier threshold law was obtained.

The convergent close-coupling method (CCC) represents another approach which has proven fairly successful for obtaining total cross sections (Bray and Stelbovics 1993, Bray 1997). This method employs a conventional coupled-state calculation augmented by pseudostates to represent continuum channels. The total inelastic cross section and the cross section for elastic scattering and excitation to any state are computed by solving the coupled-channel equations. The ionization component is extracted by subtracting the elastic and inelastic cross sections from the total cross section. The results are consistent with Wannier’s threshold law for energies above 1 eV.

The *R*-matrix methods with pseudostates (RMPS) and the variational calculations of Callaway (1991) also compute cross sections that are in agreement with the Wannier threshold law for sufficiently high energies. Very recently, the RMPS method has been investigated for energies within 0.5 eV of threshold (Scott *et al* 1997). At present only the  $^1S$  symmetry has been computed in detail. Results are encouraging and it appears that even at this energy the method agrees with the Wannier theory. These successes are important because both the CCC and RMPS are designed to treat many-electron atomic species.

The most accurate calculations in the threshold region, at both positive and negative energies, for electron impact on atomic hydrogen are those based upon the hyperspherical close-coupling expansion (Kato and Watanabe 1995, 1996, 1997). By using a large number of coupled channels, up to 900 in some cases, an accurate total wavefunction is computed at *R* of the order of 1000 au. The excitation and elastic scattering components are subtracted leaving a wavefunction representing fragmentation. This wavefunction is then fitted onto a product of a Coulomb wave and a plane wave to extract the ionization amplitude. Using this procedure, Kato and Watanabe (1995, 1996, 1997) obtained cross sections in good agreement with experiment and with the Wannier threshold law down to energies of 0.2 eV above threshold.

### 3.2. Neutral species

In this section, we return to the consideration of short-range potentials (potentials that fall off faster than  $1/r^2$ ). In particular, we will have the example of interacting neutral atoms in mind which interact via a  $1/r^6$  van der Waals potential. Many of the considerations for these systems apply equally well to interacting nucleons. In fact, two of the effects we will describe below originated in studies of nuclear structure and continue to capture interest in that field. The short-range nature of the interactions affords a considerable simplification compared to the charged particle case discussed in the last section since the adiabatic hyperspherical approach can be employed to reduce the problem to a standard multichannel scattering problem. The resulting adiabatic potentials have an effective centrifugal barrier with  $1/R^3$  and shorter-range corrections. Consequently, the asymptotic form of the three-body wavefunction can be described straightforwardly in these coordinates in terms of Bessel functions in the hyper-

radius, paralleling the treatment in section 2.5 for two bodies. The various threshold laws can thus be deduced using a Wigner-type analysis.

*3.2.1. Efimov–Thomas effect.* Efimov (1970, 1973, 1990) derived a remarkable result: three particles interacting pairwise through short-range potentials could have an infinite number of bound states—even if no two of the particles were separately bound. The condition for the existence of an infinite number of these ‘Efimov’ states is that the ratio of the two-body scattering length  $a$  to the effective range  $r_{\text{eff}}$  must be infinitely large. For large finite  $a$ , there will be a finite number of bound states, some of the higher lying of which can retain the character of an Efimov state. When  $a > r_{\text{eff}}$ , an explicit estimate of the number of such states is given by (Efimov 1970)

$$n \approx \frac{1}{\pi} \ln \frac{a}{r_{\text{eff}}}. \quad (76)$$

Efimov was explicitly considering short-range potentials, but the limit applies to zero-range potentials as well. The latter case had already been considered by Thomas (1935) and was revisited by Danilov (1961). Specifically, it was already known to Efimov that three particles interacting via attractive zero-range,  $r_{\text{eff}} \rightarrow 0$ , potentials had been shown to have an infinite number of bound states.

In the adiabatic hyperspherical approach, the Efimov effect manifests itself in the potential curve correlating to three free atoms (Macek 1986). The abundance of bound states can be readily understood as the consequence of this having an attractive  $1/R^2$  tail. This result had been found by Efimov in terms of  $R^2 = r_{12}^2 + r_{23}^2 + r_{31}^2$  and later through an analytical variational treatment in hyperspherical coordinates by Macek, who showed that the adiabatic potential asymptotically behaves as (Macek 1986)

$$U(R) \rightarrow -\frac{t^2 - \frac{1}{4}}{2\mu R^2}. \quad (77)$$

In this expression,  $t$  is the variational parameter whose value was determined to be approximately 1.006. This result was confirmed in later direct numerical calculations by Esry *et al* (1996). As discussed in section 2.4.1 and equation (21), such dipole potentials support an infinite number of bound states whose energy converges exponentially to the break-up threshold. Another property of dipole states is that their spatial extent increases exponentially with the principal quantum number, leading to the often-cited weak-binding property of Efimov states. Equation (77) holds, however, only in the limit of infinite two-body scattering length. For finite scattering lengths, the leading asymptotic correction to the non-interacting result becomes proportional to  $a/R^3$  (Macek 1986). As a result of this transition from a short-range (falling off faster than  $1/R^2$ ) potential to a dipole potential when  $a \rightarrow \infty$ , the threshold law is dramatically modified, as mentioned above, changing from the expected  $E^2$  dependence to a constant value at threshold.

We note that while it is very unlikely that the exact case of the Efimov effect will be seen, a system with a finite number of three-body bound states with Efimov-like properties can be expected to exist. The helium trimer has long been noted to be an extremely good prospect, and it has recently been shown convincingly that of the two bound states of the helium trimer, the excited state has the characteristics of an Efimov state (Esry *et al* 1996, Cornelius and Glöckel 1986, Nielsen *et al* 1998). In nuclear systems, many examples exist of the closely related phenomenon of ‘halo’ states. Many halo states are also weakly bound three-body states, the bulk of whose wavefunction lies outside the range of the two-body interactions. These are typically neutron-rich nuclei such as  $^{11}\text{Li}$  and  $^6\text{He}$  that lie along the ‘dripline’ (Fedorov *et al* 1994).

3.2.2. *Recombination.* We have thus far considered break-up processes and the associated threshold laws. In this section, we examine the time-reverse process of recombination. In particular, we consider the recombination of three neutral atoms into a diatomic molecule and a free atom. This process is of practical interest for atomic Bose–Einstein condensation experiments since neither the resulting molecule, nor the atom that receives the excess energy, remain trapped. Three-body recombination thus limits the lifetime of a condensate. Three-body recombination is also of more general interest since it is little studied as a quantum phenomenon.

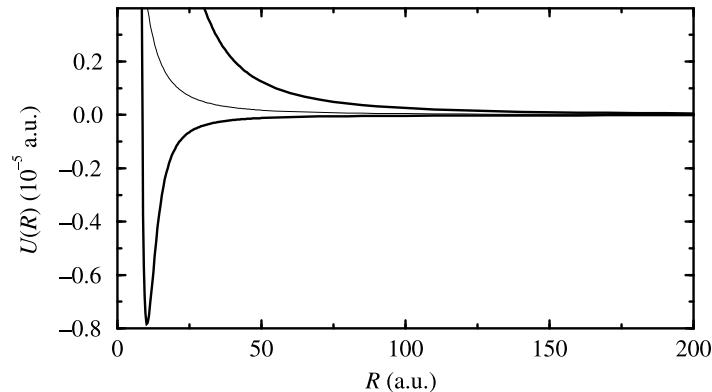


**Figure 10.** The lowest two adiabatic hyperspherical potential curves for the helium trimer (heavy full curves) are shown along with the lowest potential for three non-interacting particles (light full curve).

As for the Efimov–Thomas effect above, the adiabatic hyperspherical approach proves to be a useful tool for the analysis of recombination. Due to the short-range nature of the two-body potentials, the adiabatic potentials are also short ranged (when  $a \neq \infty$ ). We show in figure 10 an example of the adiabatic potentials for three identical bosons with total angular momentum,  $L = 0$ . We have chosen the relatively simple case of the helium trimer. The helium dimer has a single weakly bound state with a binding energy of about 1 mK, giving rise to a He–He scattering length of about 200 au. Thus, there exists only one molecular recombination channel, and the three-body continuum channel potential is more repulsive than the non-interacting curve (shown in the figure as the thin full curve). The scattering analysis mirrors that discussed for two-body scattering with the result that the cross section for recombination of three identical bosons is proportional to  $E^{-1/2}$  near threshold. This is the system most relevant to Bose–Einstein condensation. The rate, a velocity times the cross section, for recombination is a constant at threshold and is dominated by the S-wave since the rate is proportional to  $E^L$  at threshold. For fermionic systems with different permutational symmetry requirements, this threshold law must be modified. In general, these modifications will make the cross section less singular, i.e. depend on a higher power of the energy.

As demonstrated recently by Inouye *et al* (1998) (see also figure 6) two-body scattering is amenable to variations over a wide range of values using moderate magnetic fields. It is therefore interesting to study the scattering length dependence of the recombination rate. Note that here we consider the rate rather than the cross section itself. It is appropriate to use the two-body scattering length as a parameter for this three-body process since the asymptotic behaviour of both the incoming three free atom channel and the outgoing molecule plus free

atom channel potentials are determined to leading order in  $R^{-1}$  by the scattering length (Macek 1986, Nielsen *et al* 1998, Efimov 1979).

The primary scattering length dependence can be understood starting from the threshold behaviour of the inelastic scattering  $S$ -matrix element  $S_{12}$ . Near threshold,  $|S_{12}|^2$  is proportional to  $E^2$  (or  $k^4$ ). However,  $|S_{12}|^2$  is a dimensionless quantity, a probability, so that we must have  $|S_{12}|^2 \propto (ka)^4$ , given that  $a$  is the available unit of length. The recombination rate  $K$  is thus

$$K \propto k\sigma_{12} \propto k \frac{|S_{12}|^2}{k^5} \propto a^4. \quad (78)$$

This overall analytic behaviour of the rate has been found using various methods by Efimov (1979), Fedichev *et al* (1996a), Nielsen and Macek (1999) and Esry *et al* (1999). It has further been verified by direct numerical calculation of the recombination rate by Esry *et al* (1999).

The possibility exists for the  $a^4$  behaviour to be modified by quantum effects for both positive and negative  $a$  (Nielsen and Macek 1999, Esry *et al* 1999). For positive scattering lengths, the long-range coupling between the incident three-body channel and the molecular formation channel peaks around  $3a$  in the hyper-radius and leads to an interference minimum in the recombination cross section. This effect could be partially or completely washed out in the presence of several molecular bound states, however, due to the interference of multiple paths. For negative scattering lengths, when the three-body channel has a barrier, the coupling between the incident channel and the recombination channels peaks at hyper-radii within the barrier. Tunnelling resonances can thus greatly enhance the recombination rate by making it more likely for the atoms to reach the region of strong coupling. In addition, the coefficient of the overall  $a^4$  scaling is larger for negative scattering lengths since the incident channel is attractive relative to the non-interacting case. On average, the atoms penetrate further into the strong-coupling region than for positive scattering lengths, leading to their overall larger recombination rate.

#### 4. Threshold laws in lower dimensions

The phase space factor  $k$ , which forms the basic component of the Wigner laws in equation (5), is correspondingly different in lower dimensions. Thus, it is replaced by no dependence on  $k$  at all in two- and by  $1/k$  in one-dimensional problems. These are of interest because external fields sometimes lower the effective dimensions as does a strong magnetic field for electron-atom/molecule problems. The transverse motion of the electron in such a channel is quantized into the Landau levels of the magnetic field and, when only the lowest level is occupied as in the case of  $E < \hbar\omega$  where  $\omega$  is the cyclotron frequency, these dimensions are frozen out as degrees of freedom, the electron having only its residual motion in that dimension parallel to the magnetic field. Quantum dots provide another context in which the trapped electrons are effectively in lower dimensions (Livermore *et al* 1996).

The arguments alongside equations (6)–(9) can be adapted, showing a subtlety inherent to one dimension. Again, for a short-range (say, attractive potential confined to  $|x| \leq x_0$ ) potential, the  $E = 0$  Schrödinger equation for  $|x| \leq x_0$  has only the  $d^2/dx^2$  kinetic energy term with the solution

$$\Psi(E = 0) = A_1x + A_2 \quad (79)$$

with  $A_2/A_1$  insensitive to  $E$ . For  $E > 0$ , if we consider separately odd- and even-parity solutions at large  $x$ , we obtain

$$\begin{aligned} \Psi_-(E) &= \sin(kx + \delta_-) = \cos \delta_- [\sin kx + \tan \delta_- \cos kx] \\ \Psi_+(E) &= \cos(kx + \delta_+) = \cos \delta_+ [\cos kx - \tan \delta_+ \sin kx]. \end{aligned} \quad (80)$$

Continuity of solutions at  $x = 0$  with the condition of proximity to threshold,  $k \rightarrow 0$ , requires that

$$\tan \delta_- = (A_2/A_1)k \quad \tan \delta_+ = -(A_1/A_2)k \quad (81)$$

with  $\Psi(E) = k\Psi(E = 0)$  in both cases. Thus, inelastic cross sections in one dimension for either parity, are given by  $\sigma_{\text{inel}} \propto (1/k)(k)^2 \propto k$ , upon combining with the  $1/k$  of phase space. In particular, note that even-parity states also have such a  $k$  dependence, not  $1/k$ , this being associated with  $\tan \delta_+$  going to infinity as  $k \rightarrow 0$  so that  $\delta_+ \rightarrow -\pi/2$ . This, in turn, is associated with the feature that even the feeblest attractive potential supports a bound state in one dimension (not in three) and, therefore, the near-threshold continuum function in equation (81) is a sine and not a cosine function for positive parity.

Threshold laws for inelastic processes can be derived using two alternative ways: one uses the Fermi golden rule, and the other uses the Wigner concept of the reaction sphere. Of course both approaches, if used correctly, give the same results. However, application of the Fermi golden rule requires some caution. In the three-dimensional case, the plane-wave approximation for the final-state wavefunction leads to the correct energy behaviour for the reaction cross section. However, in the one-dimensional case, the plane-wave approximation gives the wrong results as discussed in the previous paragraph, giving inelastic cross sections near the threshold which diverge as  $k^{-1}$ , instead of the correct result  $\sigma \sim k$ . This behaviour was discussed in connection with the problem of electron scattering in a magnetic field by Ventura (1973) and Clark (1983). The correct threshold law for this case was derived using a wavefunction which took into account the final-state interaction. Whereas this approach is non-perturbative with respect to the final-state interaction, it still uses perturbation theory with respect to the non-diagonal part of the interaction leading to the inelastic (or reaction) process. Of course, this approach is justified in the problem of single-photon detachment when the reactive interaction (atom-photon) is much weaker than the final-state interaction (electron-atom). However, it is legitimate to ask whether the same approach would be valid in the case of a strong reactive interaction, for example in electron-impact excitation. Another example is interaction with channels other than the initial and final channel. For photodetachment in a magnetic field, this corresponds to interaction with other Landau channels in the final state. Since perturbation theory with respect to the final-state interaction fails to predict the correct threshold law in the one-dimensional case, there is reason to suspect that it might also fail with respect to the interchannel coupling.

#### 4.1. Wigner derivation

*4.1.1. Two-dimensional case.* The flux in the incident channel in two dimensions is measured per unit length rather than per unit area, so that the ‘cross section’ in this case has dimensions of length. First, we need to connect the cross section with the scattering matrix. To this end, we will consider the asymptotic behaviour of the multichannel wavefunction

$$\Psi_{fi} \sim \exp(i\mathbf{k}_i \cdot \mathbf{r})\delta_{fi} + \frac{e^{ik_f r}}{\sqrt{r}} f_{fi}(\theta) \quad (82)$$

where the ‘scattering amplitude’  $f_{fi}(\theta)$  has dimensions of the square root of length. By calculating fluxes in the incident and outgoing channels we obtain, as in three dimensions,

$$\frac{d\sigma_{fi}}{d\theta} = \frac{k_f}{k_i} |f_{fi}(\theta)|^2. \quad (83)$$

The partial-wave expansion of the incident plane wave is

$$\exp(\mathbf{i}k_i \cdot \mathbf{r}) = \sum_m \mathbf{i}^m e^{im\theta} J_m(k_i r) \quad (84)$$

and the scattering amplitude can also be expanded in  $\exp(im_f \theta)$ . The asymptotic behaviour of the radial wavefunctions is finally given as

$$\psi_{fi}(r) \sim \frac{\mathbf{i}^{m_f}}{r^{1/2}} \left[ \left( \frac{2}{\pi k_i} \right)^{1/2} \frac{e^{i\rho_i} + e^{-i\rho_i}}{2i} \delta_{fi} + e^{i(\rho_f + \pi/4)} f_{fi} \right] \quad (85)$$

where  $\rho_i = k_i r - m_i \pi/2 - \pi/4$ . Now it is convenient to introduce the transition matrix  $T_{fi}$  as

$$f_{fi} = -\frac{e^{-i\pi/4}}{2i} \left( \frac{2}{\pi k_f} \right)^{1/2} T_{fi}. \quad (86)$$

A derivation along the lines of section 2.3 gives

$$T = 2[1 + \mathbf{i}(f')^{-1}g' - \mathbf{i}(f'Rf' - f'f)^{-1}]^{-1} \quad (87)$$

or, using analytical properties of the pair  $(f, g)$ ,

$$T = 2k^m [k^{2m} + \mathbf{i}(f^{0'})^{-1}g^{0'}\chi_m(k)k^m - \mathbf{i}(f^{0'}Rf^{0'} - f^{0'}f^{0'})^{-1}]^{-1}k^m. \quad (88)$$

The  $T$ -matrix in this form is explicitly symmetric, since  $k, \chi, f^0$  and  $g^0$  are diagonal and  $R$  is symmetric.

Consider now the threshold behaviour when  $k_f \rightarrow 0$ . If  $m_f > 0$ , none of the matrix elements in the square brackets behaves singularly, and we obtain  $T_{fi} \sim k_f^{m_f}$ . However, if  $m_f = 0$ , one of the diagonal matrix elements has a logarithmic singularity,  $\ln k_f$ , so that  $T_{fi} \sim (\ln k_f)^{-1}$ . The cross section for an endothermic process behaves as

$$\sigma_{fi} \sim (\ln k_f)^{-2}. \quad (89)$$

The cross section for elastic scattering is

$$\sigma_{ff} \sim (k_f \ln^2 k_f)^{-1} \quad (90)$$

and the cross section for an exothermic reaction (superelastic scattering)

$$\sigma_{fi} \sim (k_f \ln^2 k_f)^{-1}. \quad (91)$$

**4.1.2. One-dimensional case.** The one-dimensional case requires some modifications because the matching conditions should be applied at two distances:  $x = -x_0$  and  $x_0$ . If the interaction has inversion symmetry, the treatment can be simplified, and only one boundary condition need be considered explicitly for the derivation of the threshold law (Clark 1983). Here we will consider the general case of a non-symmetric potential.

If the incident beam propagates along the  $x$ -axis in the negative direction, the matrix of the wavefunctions outside the reaction region is

$$\psi_{fi} = \psi_{ii}^- \delta_{fi} + \psi_{ff}^+ T_{fi}^{++} \quad \text{if } x > x_0 \quad (92)$$

$$\psi_{fi} = \psi_{ff}^- T_{fi}^{-+} \quad \text{if } x < -x_0 \quad (93)$$

where  $T^{++}$  and  $T^{-+}$  are reflection and transmission matrices, and  $\psi^\pm$  are diagonal matrices

$$\psi^\pm = k^{-1/2} \exp(\pm ikx). \quad (94)$$

If the incident beam propagates in the positive direction, we have instead

$$\psi_{fi} = \psi_{ii}^+ \delta_{fi} + \psi_{ff}^- T_{fi}^{--} \quad \text{if } x < -x_0 \quad (95)$$

$$\psi_{fi} = \psi_{ff}^+ T_{fi}^{+-} \quad \text{if } x > x_0. \quad (96)$$

This can be rewritten in a compact form using  $2N \times 2N$ -matrices, and a derivation along previous lines gives

$$T_{fi} \sim k_f^{1/2} \quad \text{if } i \neq f. \quad (97)$$

The case  $i = f$  requires more consideration. Consider first the case when  $k_f = 0$  exactly. Then the  $f$  channel becomes decoupled from all others, and as  $k \rightarrow 0$ , the reflection coefficient goes to  $-1$  and the transmission coefficient to 0. It is easy to see now that at small but finite  $k_f$ ,

$$T_{ff}^{++} = -1 + bk_f \quad T_{ff}^{--} = ck_f \quad (98)$$

where  $b$  and  $c$  are constants. Note that if only the  $f$  channel is open, the constant  $b$  is pure imaginary which provides conservation of probability in the channel  $f$ :  $|T_{ff}^{++}|^2 + |T_{ff}^{--}|^2 = 1$ . However, in the presence of other open channels,  $b$  has a non-zero real part and  $|T_{ff}^{++}|^2 + |T_{ff}^{--}|^2 < 1$ .

Analytical properties of the exponentials  $e^{\pm ikr_0}$  can be used to obtain the next terms of the effective range expansion of the  $T$ -matrix. The behaviour of the non-diagonal elements of the  $T$ -matrix, equation (97), leads to the following threshold law for the probability of inelastic process  $w_{fi}$ :

$$w_{fi} \sim k_f \quad (99)$$

which agrees with the earlier remark following equation (81) and with the result obtained by Clark (1983) for the process of photodetachment in a magnetic field. We note, however, that our derivation is more general, since it is non-perturbative with respect to the interchannel coupling and does not use the symmetry property of the Hamiltonian with respect to inversion. Note also that Wigner's derivation in principle cannot lead to the divergent behaviour  $w_{fi} \sim k_f^{-1}$  resulting from perturbation theory because such behaviour violates conservation of probability, while Wigner's theory is inherently unitary.

#### 4.2. Electron–molecule scattering

We have already discussed one important example related to scattering in one dimension: scattering and photodetachment in an external magnetic field. Here we will discuss other examples: electron–molecule scattering leading to formation of two heavy particles, specifically dissociative attachment and electron-impact dissociation. If the incident electron energy is large compared to the rotational spacing, these processes can be treated assuming that the molecule's orientation is fixed. Then the atomic fragments dissociate along the reaction coordinate (for example, along the internuclear axis in the case of a diatomic molecule), and the problem can be considered as one dimensional with respect to the nuclear motion. We will limit our discussion to the case of endothermic reactions, when the threshold energy is positive. According to the threshold law discussed above, the cross section for the dissociative attachment should be proportional to the relative momentum of the nuclei  $p$ ,

$$\sigma_{\text{DA}} \propto p. \quad (100)$$

Regarding dissociation, we have to consider the energy sharing between the three-dimensional electronic and the one-dimensional nuclear motion. According to the golden rule, the fourfold differential cross section is

$$d^4\sigma_{\text{diss}} \propto |\mathcal{M}|^2 \delta(E - \nu - \epsilon) d^3k dp \quad (101)$$

where  $E$  is the total energy,  $\epsilon = k^2/2$  is the electron energy in atomic units and  $\nu = D_0 + p^2/2M$  is the energy of nuclear motion, where  $D_0$  is the dissociation energy and  $M$  is the reduced mass of the molecule. According to the above discussion, the matrix element  $\mathcal{M}$  is finite at  $\epsilon = 0$ . After integrating over  $\epsilon$ , we obtain the following equation for the singly differential cross section:

$$d\sigma_{\text{diss}} \propto |\mathcal{M}|^2 (E - \nu)^{1/2} (\nu - D_0)^{-1/2} d\nu. \quad (102)$$

Now the threshold law depends critically on the threshold behaviour of  $|\mathcal{M}|$ . If we used the Born approximation for  $\mathcal{M}$ , we would obtain the cross section which is divergent at  $\nu \rightarrow D_0$ . However, as we know, the correct threshold behaviour of  $\mathcal{M}$  is

$$\mathcal{M} \propto (\nu - D_0)^{1/2} \quad (103)$$

which restores the Wigner law for  $d\sigma_{\text{diss}}$ ,

$$d\sigma_{\text{diss}} \propto (E - \nu)^{1/2} (\nu - D_0)^{1/2} d\nu. \quad (104)$$

Integrating the resulting expression over  $\nu$ , we obtain the expression for the total cross section

$$\sigma_{\text{diss}} \propto (E - D_0)^2 \quad (105)$$

which is the same as that derived for three dimensions (Rau 1984a). However, whereas the latter was derived using the density-of-states argument, our approach stresses the importance of knowledge of the correct energy dependence of the matrix element  $\mathcal{M}$ .

In practice, the cross sections for dissociative attachment and dissociation usually exhibit a behaviour which is different from that discussed above. If there is no potential barrier for the dissociative attachment reaction, its cross section starts with a finite value immediately above threshold. The singly differential dissociation cross section exhibits the Wigner behaviour with respect to the electron energy  $E - \nu$ , but it is finite at threshold with respect to  $\nu - D_0$  (Fabrikant *et al* 1991).

To interpret these deviations from the Wigner law, we have to realize that the de Broglie wavelength of the final fragments is relatively small, and their motion can be described in the quasiclassical approximation. The energy-normalized quasiclassical wavefunction can be written as

$$\psi = \left[ \frac{P}{P(R)} \right]^{1/2} \sin(S(R) + \pi/4) \quad (106)$$

where  $P(R)$  is the classical momentum as a function of the internuclear distance and  $S(R)$  is the classical action. As  $p \rightarrow 0$ ,  $\psi \propto \sqrt{p}$ , so that in the quasiclassical approximation

$$|\mathcal{M}_{\text{DA}}|^2 \propto p \quad (107)$$

and  $\sigma_{\text{DA}}$  is finite at threshold. For the singly differential dissociation cross section, we obtain

$$d\sigma_{\text{diss}} \propto (E - \nu)^{1/2} d\nu \quad (108)$$

which means that the cross section is finite at  $\nu = D_0$  and obeys the Wigner law if  $\nu \rightarrow E$ . The total dissociation cross section is proportional to  $(E - D_0)^{3/2}$ .

## 5. Conclusion

The threshold laws presented in this review encompass a vast array of phenomena in atomic and molecular physics, including one- and two-electron photodetachment, (e,2e) processes, and collisions and recombination of ultracold atoms, as well as their behaviour in external electromagnetic fields and in low dimensions. On the experimental side, energy resolution continues to improve in electronic, atomic, molecular and ionic sources. Perhaps most notably, the controlled environment of magneto-optical atom traps provides researchers with opportunities to interrogate particle interactions at energies extremely close to dissociation/recombination limits, and even to manipulate these interactions. As resolution continues to improve the threshold laws will stand at the centre of an ever-widening array of experiments. We have summarized these laws in one place to make them available for new generations of experiments, as well as to place them in the context of the prior advances of the past half-century.

## Acknowledgments

This work was initiated following a workshop on threshold phenomena in 1998 at the Institute for Theoretical Atomic and Molecular Physics. ARPR thanks Professors F H M Faisal and J Hinze and their groups at the University of Bielefeld for their hospitality and the Alexander von Humboldt Stiftung for support. IIF is grateful to E Heller for stimulating discussions on threshold laws in lower dimensions. IIF was supported by the National Science Foundation, grant nos PHY-9509265 and PHY-9801871. HRS was supported by a National Science Foundation grant to the Institute for Theoretical Atomic and Molecular Physics at the Harvard-Smithsonian Center for Astrophysics. MJC acknowledges support by the Division of Chemical Sciences, Offices of Basic Energy Sciences, Office of Energy Research, US Department of Energy. JHM is sponsored by the Division of Chemical Sciences, Office of Basic Energy Sciences, US Department of Energy, under contract no DE-AC05-96OR22464 through a grant to Oak Ridge National Laboratory, which is managed by Lockheed Martin Energy Research Corp., and by the National Science Foundation under grant no PHY-9600017. JLB was supported by the National Science Foundation.

## References

- Abraham E R I *et al* 1996 *Phys. Rev. A* **53** R3713  
—1997 *Phys. Rev. A* **55** R3299  
Balakrishnan N, Forrey R C and Dalgarno A 1998 *Phys. Rev. Lett.* **80** 3224  
Bardsley N and Mandl F 1968 *Rep. Prog. Phys.* **31** 471  
Barnea N and Novoselsky A 1998 *Phys. Rev. A* **57** 48  
Baz' A I 1957 *Zh. Eksp. Teor. Fiz.* **33** 923 (Engl. transl. 1958 *Sov. Phys.-JETP* **6** 709)  
—1959 *Zh. Eksp. Teor. Fiz.* **36** 1762 (Engl. transl. 1959 *Sov. Phys.-JETP* **9** 1256)  
Bethe H A 1949 *Phys. Rev.* **76** 38  
Boesten H M J M *et al* 1997 *Phys. Rev. A* **55** 636  
Bohn J L and Julienne P S 1997 *Phys. Rev. A* **56** 1486  
—1999 *Phys. Rev. A* **60** 414  
Bray I 1997 *Phys. Rev. Lett.* **78** 4721  
Bray I and Stelbovics A 1993 *Phys. Rev. Lett.* **70** 746  
Bryant H C *et al* 1977 *Phys. Rev. A* **38** 228  
Buckman S J *et al* 1983 *J. Phys. B: At. Mol. Phys.* **16** 4039  
Burke J P Jr, Greene C H and Bohn J L 1998 *Phys. Rev. Lett.* **81** 3355  
Burke J P Jr *et al* 1997 *Phys. Rev. A* **55** R2511  
—1999 *Phys. Rev. A* **60** 4417

- Callaway J 1991 *Phys. Rev. A* **44** 2192  
Cavagnero M 1994 *Phys. Rev. A* **50** 2841  
Clark C W 1979 *Phys. Rev. A* **20** 1875  
—1983 *Phys. Rev. A* **28** 83  
Crawford O H and Garrett W R 1977 *J. Chem. Phys.* **66** 4968  
Crothers D S F 1986 *J. Phys. B: At. Mol. Phys.* **19** 463  
Crothers D S F and Lennon D J 1988 *J. Phys. B: At. Mol. Opt. Phys.* **21** L409  
Cornelius T and Glöckle W 1986 *J. Chem. Phys.* **85** 3906  
Courteille Ph *et al* 1998 *Phys. Rev. Lett.* **81** 69  
Cvejanovic S and Read F H 1974 *J. Phys. B: At. Mol. Phys.* **7** 1841  
Cvejanovic S, Shiell R and Reddish T J 1995 *J. Phys. B: At. Mol. Opt. Phys.* **28** L707  
Damburg R J 1968 *J. Phys. B: At. Mol. Phys.* **1** 1001  
Danilov G S 1961 *Zh. Eksp. Teor. Fiz.* **40** 498 (Engl. transl. 1961 *Sov. Phys.—JETP* **13** 349)  
Demkov Y N and Osherov V I 1967 *Zh. Eksp. Teor. Fiz.* **53** 1589  
DeMarco B *et al* 1999 *Phys. Rev. Lett.* **82** 4208  
Dodd R J *et al* 1996 *Phys. Rev. A* **54** 661  
Donahue J B *et al* 1982 *Phys. Rev. Lett.* **48** 1538  
Dulieu O, Julienne P and Weiner J 1994 *Phys. Rev. A* **49** 607  
Edwards M and Burnett K 1995 *Phys. Rev. A* **51** 1382  
Efimov V 1970 *Phys. Lett. B* **33** 563  
—1973 *Nucl. Phys. A* **210** 157  
—1979 *Yad. Fiz.* **29** 1058 (Engl. transl. 1979 *Sov. J. Nucl. Phys.* **29** 546)  
—1990 *Comment. Nucl. Part. Phys.* **19** 271  
Engelking P C 1982 *Phys. Rev. A* **26** 740  
Engelking P C and Herrick D R 1984 *Phys. Rev. A* **29** 2425  
Erdelyi F, Hettinger O, Magnus W and Triocomi F G 1953 *Higher Transcendental Functions* vol II (New York: McGraw-Hill)  
Esry B D, Burke J P Jr and Greene C H 1999 *Phys. Rev. Lett.* **83** 1751  
Esry B D, Lin C D and Greene C H 1996 *Phys. Rev. A* **54** 394  
Fabrikant I I 1977 *Zh. Eksp. Teor. Fiz.* **73** 1317 (Engl. transl. 1977 *Sov. Phys.—JETP* 1977 **46** 693)  
—1978 *J. Phys. B: At. Mol. Phys.* **11** 3621  
—1983 *J. Phys. B: At. Mol. Phys.* **16** 1269  
—1984 *J. Phys. B: At. Mol. Phys.* **17** 4223  
—1996 *Comment. At. Mol. Phys.* **32** 267  
Fabrikant I I, Kalin S A and Kazansky A K 1991 *J. Chem. Phys.* **95** 4966  
Fabrikant I I and Wilde R S 1999 *J. Phys. B: At. Mol. Opt. Phys.* **32** 235  
Fano U 1974 *J. Phys. B: At. Mol. Phys.* **7** L401  
—1983 *Rep. Prog. Phys.* **46** 97  
Fano U and Rau A R P 1985 *Comment. At. Mol. Phys.* **16** 241  
—1986 *Atomic Collisions and Spectra* (Orlando, FL: Academic)  
—1996 *Symmetries in Quantum Physics* (San Diego, CA: Academic)  
Feagin J M 1984 *J. Phys. B: At. Mol. Phys.* **17** 2433  
—1995 *J. Phys. B: At. Mol. Opt. Phys.* **28** 1495  
Feagin J M and Filipczyk R D 1990 *Phys. Rev. Lett.* **64** 384  
Fedichev P O, Reynolds M W and Shlyapnikov G V 1996a *Phys. Rev. Lett.* **77** 2921  
Fedichev P O *et al* 1996b *Phys. Rev. Lett.* **77** 2913  
Fedorov D V and Jensen A S 1993 *Phys. Rev. Lett.* **71** 4103  
Fedorov D V, Jensen A S and Riisager K 1994 *Phys. Rev. Lett.* **73** 2817  
Fermi E and Teller E 1947 *Phys. Rev.* **72** 399  
Flambaum V V, Gribakin G F and Harabati C 1999 *Phys. Rev. A* **59** 1998  
Forrey RC *et al* 1998 *Phys. Rev. A* **58** R2645  
Frey M T *et al* 1994 *Phys. Rev. A* **50** 3124  
—1995 *Phys. Rev. Lett.* **75** 810  
Gailitis M 1963 *Zh. Eksp. Teor. Fiz.* **44** 1974 (Engl. transl. 1963 *Sov. Phys.—JETP* **17** 1328)  
—1970 *Teor. Mat. Fiz.* **3** 364  
—1982 *J. Phys. B: At. Mol. Phys.* **15** 3423  
Gailitis M and Damburg R 1963 *Proc. R. Soc.* **82** 192  
Gao B 1999 *Phys. Rev. A* **59** 2778

- Greene C H, Fano U and Strinati G 1979 *Phys. Rev. A* **19** 1485  
Greene C H and Rau A R P 1982 *Phys. Rev. Lett.* **48** 533  
———1983 *J. Phys. B: At. Mol. Phys.* **16** 99  
———1985 *Phys. Rev. A* **32** 1352  
Gribakin G F and Flambaum V V 1993 *Phys. Rev. A* **48** 546  
Grujić P 1981 *J. Phys. B: At. Mol. Phys.* **15** 1913  
Harris P G *et al* 1990 *Phys. Rev. Lett.* **65** 309  
Herrick D R 1975 *Phys. Rev. A* **12** 413  
Hill S B *et al* 1996 *Phys. Rev. A* **53** 3348  
Hinckelman O and Spruch L 1971 *Phys. Rev. A* **3** 642  
Hino K and Macek J H 1996 *Phys. Rev. Lett.* **77** 4310  
Holzwarth N A 1973 *J. Math. Phys.* **14** 191  
Hotop H *et al* 1995 *The Physics of Electronic and Atomic Collisions* ed L J Dube *et al* (New York: AIP) p 267  
Huang K and Yang C N 1957 *Phys. Rev.* **105** 767  
Ihra W *et al* 1997 *Phys. Rev. Lett.* **78** 4027  
Inouye S *et al* 1998 *Nature* **392** 151  
Jackson R L, Zimmermann A H and Brauman J I 1979 *J. Chem. Phys.* **71** 2088  
Jakubassa-Amundsen D and Macek J M 1989 *J. Phys. A: Math. Gen.* **22** 4151  
Julienne P S 1996 *J. Res. Natl Inst. Stand. Technol.* **101** 487  
Julienne P S *et al* 1997 *Phys. Rev. Lett.* **78** 1880  
Kato D and Watanabe S 1995 *Phys. Rev. Lett.* **74** 2443  
———1996 *J. Phys. B: At. Mol. Opt. Phys.* **29** L779  
———1997 *Phys. Rev. A* **56** 3687  
Kazansky A K, Bogdanovich P O and Ostrovsky V N 1997 *J. Phys. B: At. Mol. Opt. Phys.* **30**  
Kazansky A K and Ostrovsky V N 1992 *J. Phys. B: At. Mol. Opt. Phys.* **25** 2121  
———1994 *J. Phys. B: At. Mol. Opt. Phys.* **27** 447  
Klar H 1981 *J. Phys. B: At. Mol. Phys.* **14** 3255  
Klar H and Schlecht W 1976 *J. Phys. B: At. Mol. Phys.* **9** 1699  
Kokkelmans S J J M F, Boesten H M J M and Verhaar B J 1997 *Phys. Rev. A* **55** R1589  
Kuchiev M Yu and Ostrovsky V N 1998 *Phys. Rev. A* **58** 321  
Lablanquie P *et al* 1990 *Z. Phys. D* **16** 77  
Landau L D and Lifshitz E M 1977 *Quantum Mechanics, Non-Relativistic Theory* (Oxford: Pergamon)  
Langer R E 1937 *Phys. Rev.* **51** 669  
Lee T D, Huang K and Yang C N 1957 *Phys. Rev.* **106** 1135  
Levy B and Keller J 1963 *J. Math. Phys.* **4** 54  
Lin C D 1995 *Phys. Rep.* **257** 1  
Livermore C *et al* 1996 *Science* **274** 1332  
Loughan A M and Crothers D S F 1997 *Phys. Rev. Lett.* **79** 4966  
Lubell M S *et al* 1977 *Phys. Rev. Lett.* **39** 334  
Lykke K R, Mead R D and Lineberger W C 1984 *Phys. Rev. Lett.* **52** 2221  
Macek J H 1968 *J. Phys. B: At. Mol. Phys.* **1** 831  
———1986 *Z. Phys. D* **3** 31  
———1990 *Phys. Rev. A* **41** 1361  
Macek J H and Ovchinnikov S Y 1996 *Phys. Rev. A* **54** 1  
Marinescu M and Dalgarno A 1995 *Phys. Rev. A* **52** 311  
Marinescu M, Sadeghpour H R and Dalgarno A 1994 *Phys. Rev. A* **49** 982  
Marinescu M and You L 1998 *Phys. Rev. Lett.* **81** 4596  
Mott N F and Massey H S W 1965 *The Theory of Atomic Collisions* (Oxford: Clarendon)  
Moxom J, Ashley P and Laricchia G 1996 *Phys. Rev. Lett.* **77** 1250  
Myatt C J *et al* 1997 *Phys. Rev. Lett.* **78** 586  
Napolitano R *et al* 1994 *Phys. Rev. Lett.* **73** 1352  
Nath P and Shaw G L 1965 *Phys. Rev. B* **138** 702  
Newbury N R, Myatt C J and Wieman C E 1995 *Phys. Rev. A* **51** R2680  
Newton R G 1966 *Scattering Theory of Waves and Particles* 2nd edn (New York: Springer)  
Nielsen E, Fedorov D V and Jensen A S 1998 *J. Phys. B: At. Mol. Opt. Phys.* **31** 4085  
Nielsen E and Macek J H 1999 *Phys. Rev. Lett.* **83** 1566  
Nikitin S I and Ostrovsky V N 1978 *J. Phys. B: At. Mol. Phys.* **11** 1681  
O'Malley T F 1964 *Phys. Rev.* **134** A1188

- O'Malley T F, Spruch L and Rosenberg L 1961 *J. Math. Phys.* **2** 491
- Ovchinnikov S Y 1990 *Phys. Rev. A* **42** 3865
- Peach G 1979 *J. Phys. B: At. Mol. Phys.* **12** L13
- Peterkop R 1971 *J. Phys. B: At. Mol. Phys.* **4** 513
- Pindzola M S and Robicheaux F 1998 *Phys. Rev. A* **57** 318
- Poelstra K A, Feagin J M and Klar H 1994 *J. Phys. B: At. Mol. Opt. Phys.* **27** 781
- Rau A R P 1971 *Phys. Rev. A* **4** 207
- 1976 *J. Phys. B: At. Mol. Phys.* **9** L283
- 1984a *Comment. At. Mol. Phys.* **14** 285
- 1984b *Phys. Rep.* **110** 369
- Read F H 1984a *J. Phys. B: At. Mol. Phys.* **17** 3965
- 1984b *Electron Impact Ionization* ed G H Dunn and T Mark (New York: Springer) pp 42–86
- Roberts J L *et al* 1998 *Phys. Rev. Lett.* **81** 5109
- Rosenberg L 1988 *Phys. Rev. A* **57** 1862
- Ross M H and Shaw G L 1961 *Ann. Phys.* **13** 147
- Rost J M 1994 *Phys. Rev. Lett.* **72** 1998
- Rost J M and Wintgen D 1996 *Europhys. Lett.* **35** 19
- Rudge M R H and Seaton M J 1965 *Proc. R. Soc. A* **283** 262
- Sadeghpour H R and Greene C H 1996 *Bull. Am. Phys. Soc.* **43** 1251
- Schramm *et al* 1999 *J. Phys. B: At. Mol. Opt. Phys.* **32** 2153
- Scott M P *et al* 1997 *J. Phys. B: At. Mol. Opt. Phys.* **30** L309
- Seaton M J 1983 *Rep. Prog. Phys.* **46** 167
- Shakeshaft R 1972 *J. Phys. B: At. Mol. Phys.* **5** L115
- Slater J, Read F H, Novick S E and Lineberger W C 1978 *Phys. Rev. A* **17** 201
- Smith F T 1960 *Phys. Rev.* **120** 1058
- 1962 *J. Math. Phys.* **3** 735
- Spruch L, O'Malley T F and Rosenberg L 1960 *Phys. Rev. Lett.* **5** 347
- Stwalley W C 1976 *Phys. Rev. Lett.* **37** 1628
- Temkin A 1982 *Phys. Rev. Lett.* **51** 669
- 1984 *Phys. Rev. A* **30** 2737
- Tiesinga E, Verhaar B J and Stoof H T C 1993 *Phys. Rev. A* **47** 4114
- Tiesinga E *et al* 1996 *J. Res. Natl Inst. Stand. Technol.* **101** 505
- Thomas L H 1935 *Phys. Rev.* **47** 903
- Thorsheim H R, Weiner J and Julienne P S 1987 *Phys. Rev. Lett.* **58** 23
- Tsai C C *et al* 1997 *Phys. Rev. Lett.* **79** 1245
- van Vleck J M 1923 *Proc. Acad. Natl Sci. USA* **14** 178
- Ventura J 1973 *Phys. Rev. A* **8** 3021
- Vuletić V *et al* 1999 *Phys. Rev. Lett.* **82** 1406
- Wannier G H 1953 *Phys. Rev.* **90** 817
- Weiner J *et al* 1999 *Rev. Mod. Phys.* **71** 1
- Wigner E P 1948 *Phys. Rev.* **73** 1002
- Williams C J *et al* 1999 *Phys. Rev. A* **60** 4427